TIN(IV) OXIDE COATED GOLD NANOPARTICLES: SYNTHESIS,
CHARACTERIZATION AND INVESTIGATION OF SURFACE
ENHANCED RAMAN SCATTERING ACTIVITIES

A THESIS SUBMITTED TO
THE GRADUATE SCHOOL OF NATURAL AND APPLIED SCIENCES
OF
MIDDLE EAST TECHNICAL UNIVERSITY

BY

AYLİN ELÇİ

IN PARTIAL FULFILLMENT OF THE REQUIREMENTS
FOR
THE DEGREE OF MASTER OF SCIENCE
IN
CHEMISTRY

SEPTEMBER 2017

Approval of the thesis:

TIN(IV) OXIDE COATED GOLD NANOPARTICLES: SYNTHESIS, CHARACTERIZATION AND INVESTIGATION OF SURFACE ENHANCED RAMAN SCATTERING ACTIVITIES

submitted by **AYLİN ELÇİ** in partial fulfillment of the requirements for the degree of **Master of Science in Chemistry Department, Middle East Technical University** by,

Prof. Dr. Gülbin Dural Ünver _____
Dean, Graduate School of **Natural and Applied Sciences**

Prof. Dr. Cihangir Tanyeli _____
Head of Department, **Chemistry Department, METU**

Assoc. Prof. Dr. Emren Nalbant Esentürk _____
Supervisor, **Chemistry Department, METU**

Examining Committee Members:

Prof. Dr. Nurşen Altuntaş Öztaş _____
Chemistry Dept., Hacettepe University

Assoc. Prof. Dr. Emren Nalbant Esentürk _____
Chemistry Dept., METU

Prof. Dr. Ayşen Yılmaz _____
Chemistry Dept., METU

Assoc. Prof. Dr. Gülay Ertaş _____
Chemistry Dept., METU

Prof. Dr. Ali Çırpan _____
Chemistry Dept., METU

Date: 08.09.2017

I hereby declare that all information in this document has been obtained and presented in accordance with academic rules and ethical conduct. I also declare that, as required by these rules and conduct, I have fully cited and referenced all material and results that are not original to this work.

Name, Last name : Aylin ELÇİ

Signature :

iv

ABSTRACT

TIN(IV) OXIDE COATED GOLD NANOPARTICLES: SYNTHESIS, CHARACTERIZATION AND INVESTIGATION OF SURFACE ENHANCED RAMAN SCATTERING ACTIVITIES

Elçi, Aylin

M. S., Department of Chemistry

Supervisor: Assoc. Prof. Dr. Emren Nalbant Esentürk

September 2017, 75 pages

Noble metal nanoparticles (i.e. gold (Au) and silver (Ag)) have received enormous attention due to their superior optical properties related to localized surface plasmon resonance (LSPR) and their potential applications in sensing, imaging, catalysis and optoelectronic devices. In particular, the ones with anisotropic morphologies have attracted intense interest from the researchers because of their superior optoelectronic properties. High electromagnetic field forms on the nanoparticle surface. The intensity of this field is even higher on the edges and/or tips of the nanoparticles with sharp features. The molecules, which are adsorbed or in close proximity in these regions are polarized. This provides detection of molecules in trace amount by spectroscopic techniques such as surface-enhanced Raman scattering (SERS). Because of all these reasons noble metal nanoparticles with anisotropic morphologies are fascinating candidates as SERS substrates and they are subject of a very active research area.

However, agglomeration tendency of noble metal nanoparticles in harsh mediums restrict their application areas. Coating these particles with optically transparent and semiconductive materials (e.g. SnO_2, SiO_2, and TiO_2) make them more durable in harsh conditions while protecting their morphologies and optical properties.

In this study, Au nanoparticles in three different morphology (star, rod, sphere) have been synthesized, and coated with tin (IV) oxide (SnO_2) layer to obtain hybrid systems in the core-shell structure. Au nanoparticles were synthesized based on a method called *"seed-mediated growth method"*. The SnO_2 coating was performed by using a simple hydrothermal-based method. The synthesized hybrid systems have been fully characterized by a combination of UV-vis spectroscopy, transmission electron microscope (TEM) and energy-dispersive X-ray (EDX) studies, scanning electron microscope (SEM), X-Ray diffraction (XRD) and Fourier transform infrared (FTIR) spectroscopy. The characterization studies showed that Au nanoparticles with three different morphology were successfully coated with SnO_2 layer. Among them, SnO_2 coated Au nanostar hybrid system was synthesized for the first time in this study. The potential use of the Au nanostar-SnO_2 core-shell system as SERS substrate was also investigated by using crystal violet (CV) as a probe molecule. The SERS studies showed that SERS activity of Au nanostars remains after coating them with SnO_2 and the new hybrid system is very promising to be used as a SERS substrate.

Keywords: Gold nanoparticles, gold nanostars, core-shell structure, SnO_2-coated nanoparticles, surface enhanced Raman scattering (SERS).

ÖZ

KALAY(IV) OKSİT KAPLI ALTIN NANOPARÇACIKLAR: SENTEZ, KARAKTERİZASYON VE YÜZEYDE GÜÇLENDİRİLMİŞ RAMAN SAÇILMASI AKTİFLİĞİNİN ARAŞTIRILMASI

Elçi, Aylin

Yüksek Lisans, Kimya Bölümü

Tez Yöneticisi: Doç. Dr. Emren Nalbant Esentürk

Eylül 2017, 75 sayfa

Soy metal nanoparçacıklar (örneğin; altın (Au) ve gümüş (Ag)), lokalize yüzey plazmon rezonansına (LSPR) ek olarak, algılama, görüntüleme, katalizör ve optoelektronik cihazlardaki potansiyel uygulamaları ile ilgili eşsiz optik özelliklerinden dolayı büyük ilgi görmektedir. Özellikle anizotropik morfolojilere sahip olan parçacıklar, üstün optoelektronik özellikleri sayesinde araştırmacıların yoğun ilgisini çekmektedirler. Nanoparçacık yüzeyinde oluşan yüksek elektromanyetik alanın yoğunluğu, özellikle nanoparçacıkların köşelerinde ve keskin hatlara sahip olan parçacıkların sivri uçlarında daha fazladır. Bu bölgelerde ya da çok yakınlarında tutunan moleküllerin polarize olması spektroskopik tekniklerle, örneğin yüzeyde güçlendirilmiş Raman saçılması (SERS) gibi, eser miktarda molekül tespit edilmesini sağlar. Bu sebeplerden dolayı, SERS substratları için mükemmel aday olmuşlardır ve oldukça aktif bir araştırma alanına sahiptirler.

Bununla birlikte, soy metal nanoparçacıkların bazı koşullarda topaklanma eğilimi göstermesi, uygulama alanlarını kısıtlamaktadır. Bu parçacıkları optik olarak şeffaf ve yarı iletken malzemeler (örn., SnO_2, SiO_2 ve TiO_2) ile kaplamak, morfolojilerini ve optik özelliklerini koruyarak onları zor koşullarda daha dayanıklı hale getirir. Bu çalışmada, Au nanoparçacıkların üç farklı morfolojisi (yıldız, çubuk, küre) "çekirdek büyütme metodu" ile sentezlenmiş ve bu parçacıklar "basit hidrotermal tabanlı metot" ile kalay (IV) oksit (SnO_2) tabakasıyla kaplanarak çekirdek-kabuk yapısında hibrit sistemler elde edilmiştir. Sentezlenen hibrit nanoparçacıkların yapısal ve optik özellikleri, spektroskopik ve mikroskopik analiz yöntemleri; taramalı elektron mikroskopisi (SEM), geçirimli elektron mikroskopisi (TEM), ultraviyole ve görünür ışık soğurma spektroskopisi (UV-vis), X-ışını kırınımı (XRD), Fourier dönüşümlü kızılötesi spektroskopisi (FTIR) kullanılarak karakterize edilmiştir. Karakterizasyon çalışmaları üç farklı morfolojiye sahip Au nanoparçacıkların SnO_2 ile başarılı bir şekilde kaplandığını göstermektedir. Bu parçacıklar arasında, SnO_2 kaplı Au nanoyıldız melez sistemi ilk kez bu çalışmada sentezlenmiştir. Au nanoyıldız çekirdek-SnO_2 kabuk sistemin SERS substratı olarak potansiyel kullanımı kristal viyole algılayıcı molekülü kullanılarak incelenmiştir. SERS çalışmaları, Au nanoparçacıkların SnO_2 ile kaplandıktan sonra SERS aktivitesini koruduğunu ve elde edilen yeni melez sistemin SERS substratı olarak kullanımının oldukça umut verici olduğunu göstermektedir.

Anahtar Kelimeler: Altın nanoparçacıklar, altın nanoyıldızlar, çekirdek-kabuk yapısı, SnO_2-kaplı nanoparçacıklar, yüzeyde güçlendirilmiş Raman saçılması.

To My Family

ACKNOWLEDGEMENTS

TABLE OF CONTENTS

LIST OF FIGURES

LIST OF ABBREVIATIONS

ca.: Circa

Crystal Violet : CV

CTAB: hexadecyltrimethylammoniumbromide

°C: degrees Celsius

DI: Deionized water

EDX: Energy Dispersive X-ray Spectroscopy

EF: Enhancement Factor

et al: et alii (and others)

FTIR: Fourier Transform Infrared Spectroscopy

LSPR: Localized Surface Plasmon Resonance

µL: Microliter

mL: Milliliter

mol: Mole

nm: Nanometer

PVP: Polyvinyl pyrrolidone

rpm: revolutions per minute

SEM: Scanning Electron Microscope

SERS: Surface Enhanced Raman Scattering

SPR: Surface Plasmon Resonance

TEM: Transmission Electron Microscope

UV-vis: Ultraviolet-visible Spectroscopy

XRD: X-Ray Diffraction

CHAPTER 1

INTRODUCTION

1.1. Motivation for the Study

Metal nanoparticles with different size, shape and chemical properties are attracting great deal of attention due to their special chemical, electronic, optical properties. The possibility of controlling these properties to fit into particular application has become main goal of the research in this area.[1-3]

Among all the metal nanoparticles noble metal ones are particularly interesting. This is mostly because of their special optoelectronic properties that led them to be used in various areas of nanotechnology. Noble metals in nano scale have wonderful colors signifying their unique optical properties. These colors result from their strong surface plasmon resonance absorption in the visible region and differ with nanoparticles' structural properties. This led to possibility to tune their optical properties by modifying the structural properties such as size, shape and surface characteristics. Strong electromagnetic field forms at the edge and/or tips of the noble metal nanoparticles with structures that have sharp features. This electromagnetic field can interact with a molecule adsorbed on the metal surface, polarize it and led to detection of the molecule by spectroscopic techniques such as Raman spectrometer.[3-6]

Surface characteristics of nanoparticles are also very important for their stability, reactivity, optical and electronic properties. Besides changes on nanoparticles' morphology, intellectual manipulations on their surface characteristics can also

improve their functionalities for a desired application. Nanoparticle surface functionalization can be done by coating them with a layer of various polymers, biofunctional molecules, different metal or metal oxide to produce core-shell hybrid nanostructures.

One of the important reasons to coat nanoparticles with soft polymeric or hard inorganic materials is to enhance their stability since particles in nanoscale suffer from coagulation. Because all application areas of nanotechnology require nanoparticles to be stable for reproducible and reliable results. In particular, noble metal nanoparticles generally have poor stability and tendency to aggregate in certain harsh medium. Aggregation of noble metal nanoparticles result in the uncontrollable changes in their optical properties and prevent their use in applications where these properties are very crucial.[7-9] Up until now various coating-materials such as metal oxides, silica or polymers have been used to improve their stability. Among these materials SiO_2 and TiO_2 coated metal nanoparticles are attracting much attention since they have the advantage of being transparent for wavelengths in visible region.[8,9] This kind of coating provides the preservation of optical properties served by the noble metal nanoparticle core.[7,9,10] Therefore, literature is quite rich on examples of noble metal nanoparticles coated with SiO_2.[11,12,13] However, a study by Lee et. al revealed that SnO_2 coated Au nanoparticles have significantly higher stability at high pH media compared to SiO_2 coated ones.[7] The study shows higher tendency of Au nanoparticle core - SiO_2 shell system to aggregate in aqueous, slightly basic medium. This limits their various potential applications. Therefore, coating Au nanoparticles with SnO_2 have become attractive way to make them more stable.[7] Up until now only Au nanoparticles with spherical and rod-shape have been coated with SnO_2.[7,9,10] However, to the best of our knowledge, SnO_2 coated Au nanostars which have superior optical properties compared to rods and spheres have not been reported, yet.

In this study, SnO_2 coated star-shaped Au nanoparticles were synthesized along with the spherical and rod shaped ones by simple hydrothermal-based method in aqueous

medium. The potential use of Au nanostar-SnO$_2$ hybrid structure in sensing application was also investigated by SERS studies. The remained SERS activity of Au nanostars after SnO$_2$ coating make the new hybrid system very promising for other potential applications where the optical properties are needed such as photovoltaic devices and imaging.[7,14]

1.2. Nanoparticles

Nanoparticle is defined as aggregation of atoms or molecules with the radius between *1 and 100 nm* and made of 10- 10^5 atoms *(1 nanometer (nm) =10^{-9} meters, an atom is about 10^{-10} meters).* They exhibit properties between molecule and bulk materials on account of its critical dimension in this range. When the size of materials is reduced to nano-scale, their characteristics show dramatic changes and new properties arise compared to their bulk constituents.[15,16,17]

It is expected that nanoparticles exhibit some special properties different from the bulk-size materials. For example, the bulk size of Au, which has different color from that of the nanosize, is reflective in the visible wavelength range, but Au in the nanosize absorbs light. Because band gap of the material changes while approaching to nanoscale from bulk form.[17,18] Band gap is an energy range without including any electron states and related to the electrical property of a material in nanoscale. It increases with decreasing metal size. As a result, the conductivity properties of materials are changed. For example, a conductive material becomes semiconductive or a semiconductor material can change to insulator.[19,20]

Nanoparticles have been considered as promising materials for catalysis due to their unique large surface-to-volume ratios. Catalytic activity depends usually on the surface of material. Catalytic activity of the metal nanoparticles increases with increasing the surface-to-volume ratio. Also, the size of the nanoparticle is inversely proportional with the surface area to the volume ratio of the particle and one of the most important factors to affect the catalytic activity. As nanoparticle size decreases,

catalytic activity increases.[21] These special optical, electronic, catalytic properties of nanoparticles lead them to be used in wide variety of fields such as chemical, biomedical, photovoltaics, sensing, imaging, catalysis etc.[22,23]

1.3. Noble Metal Nanoparticles and Their Optical Properties

Among all metal nanoparticles noble metal ones (i.e. Au and Ag) have received a great deal of attention for last couple of decades because of their special optoelectronic properties.

Noble metals in nanoscale have bright colors associated with their distinctive optical properties. These properties led them to be used as coloring materials in ceramics and paintings in ancient times. About 150 years ago, Michael Faraday has explained the source of their beautiful colors as the interaction between light and matter. He stated that the interaction of light with matter can be observed as scattering and absorption of light. As a result, the source of the brilliant colors of noble metal nanoparticles has been understood to be owing to their unique optical properties that can be changed with size, shape, chemical identity and variety of their potential application areas.[9,19,24] More currently, the discovery of new analysis techniques has helped researchers to understand the optical and many other properties of nanoparticles better.[19]

Noble metal nanoparticles absorb different wavelengths in the visible and near-infrared region of the spectrum due to their size, shape, aggregation state and local environment of the nanoparticles.[20] For instance, the color of Au spheres is red and silver one is yellow.[17,19,25,26] It is observed that the color of the noble metal nanoparticles is caused by surface plasmon oscillation. It is defined as the collective oscillation of the electrons in the conduction band of the metal nanoparticles.[19] When the nanoparticles' size is quite smaller than the wavelength of incident light, resonance condition occurs. It created a surface interaction that the free electrons of the Ag and Au nanoparticles move through the particles freely. When the light passes through the nanoparticle, the electrons are polarized at the surface of the particle and this lead to

an electromagnetic field. The size of noble metal nanoparticles is much smaller than the visible light's wavelength which causes resonance condition. The collective oscillation of metal electrons in the conduction band occurs by means of the frequency of light in resonance with the surface plasmon oscillation. This is called as the localized surface plasmon resonance (LSPR)[19,25,27] (Figure.1).
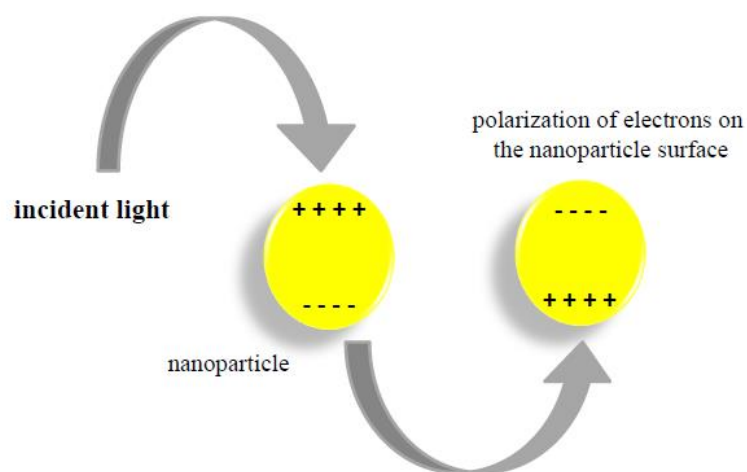
Figure 1.1. Surface plasmon resonance (SPR) condition for spherical nanoparticle

LSPR of the noble metal nanoparticles, typically Au and Ag, is observed in the visible range of the spectrum which causes some special optical properties. SPR condition brings about strong absorption of light. It changes with shape and size of the nanoparticles and also dielectric constant of the surrounding medium.[19,20,25,27-32]

Hence, changing their size and shape has an impact upon tuning their optical properties.[33-37] For instance, the optical properties of Au nanoparticles with anisotropic morphologies are better than that of spherical ones. In particular, the ones

having branched morphologies exhibit strong light absorption in the visible and near IR range. Because their sharp tips generate strong electric field, these morphologies are especially very useful for sensing, imaging, photonics, electronics and biomedical applications.[3,5,6]

Mie theory, which is an electromagnetic field theory of spherical nanoparticles, explains the optical properties of metal particles, in particular Ag and Au ones. This theory describe the size dependence of localized surface plasmon resonances, red shifts and broadening of the dipole plasmon resonance as particle size is increased, as well as the appearance of quadrupole and higher resonance contributions. As spherical metal particles come to nanoscale in form of rods, triangular prisms or disks, surface plasmon resonances are affected. Typically, plasmon bands red shift and even split into distinctive dipole and quadrupole plasmon modes. These special optical and electrical properties of nanoparticles paves the way for possible applications in surface enhanced Raman spectroscopy (SERS), electronics and biosensors.[26,38,39]

Among all the potential applications of noble metal nanoparticles surface enhanced Raman scattering (SERS) spectroscopy has received much attention due to its use as a sensitive technique for sensing and imaging. The aforementioned optical properties of noble metal nanoparticles make them commonly used SERS substrates. In particular, the noble metal nanoparticles with anisotropic morphologies have higher capabilities of enhancing Raman signals due to their sharp corners and tips which produce strong electromagnetic field. There are two effects considered as the reason for the enhanced Raman signal. The first one is *chemical enhancement* which depends on the nature of the molecule and its polarizability. Molecules with delocalized electrons have high polarizability potentials by forming charge-transfer complex with the metal surface. These kinds of molecules demonstrate strong Raman enhancement. Second effect is called as *electromagnetic enhancement*. It results from the formation of electromagnetic field on the nanoparticle surface. As explained above, the interaction of incoming light with the metal surface cause the formation of strong electromagnetic field on nanoparticle surface. The strength of this field is higher at the edge and/or tips

6

of nanoparticles with sharp features. The molecules, which are adsorbed on these points or in close proximity to the junction between two nanoparticles, are mostly affected by this field and highly polarized. As a result, their Raman signals are strongly enhanced.[1,26,38-41]

The literature examples of the utility of noble metal nanoparticles as SERS substrates are continuously increasing.[1,19,42,43-46] For instance, the study of Joseph et al. revealed that large size nanoparticles have more tendencies to form agglomeration which causes strongly enhanced SERS signals due to increasing the electromagnetic enhancement with the size of the Au nanospheres.[47] Sun and coworkers studied that the encapsulation of Au nanorods with polydopamine were used as multifunctional photothermal agents. Due to the strong SERS activity of Au nanorods they achieve accurate cancer cell detection by SERS imaging.[48] In addition, Yang et al. synthesized Au nanorod/nanosphere satellites through base pairing characteristic of DNA. These substrates exhibited high sensitivity for SERS-based detection of CV (crystal violet) due to obtained hot spots between Au nanospheres and nanorods. As a result, they suggested that these satellites have utility for SERS-based biomedical applications.[49]

On the other hand, the theoretical study of Nikoobakht and El Sayed revealed that the SERS intensity for probe molecule, 2-aminothiophenol (2-ATP), adsorbed on surfaces covered with aggregated Au nanorods were stronger than that covered with aggregated Au nanospheres in the same conditions.[42] Also, Au nanostars have been reported to enhance Raman signals of different probe molecules (i.e. 2-mercaptopyridine, crystal violet) strongly and have great potentials to be used as SERS substrates. This study also showed that nanostars have higher SERS activities compared to spherical and rod-shaped nanoparticles.[1] The promising results of the research of Au and Ag nanoparticles substrates by Herrera and coworkers were obtained in SERS-based detection of the 4-Aminobenzebethiol (4-ABT), probe molecule, so these substrates could contribute development of novel micro sensors.[50] The particle size and shape play an important role in acquired SERS intensity. The study of Stamplecoskie and Scaiano was achieved a maximum SERS intensity of R6G molecules with changing the size of Ag nanospheres.[51] Demirtas et al. investigated the effect of anisotropic

shape silver nanoparticles and verified strongly enhanced SERS signals of detected crystal violet and brilliant cresyl blue molecules by Ag nanowires.[52] Also, Au and Ag nanoparticles are cooperatively studied as substrates in many sensing applications. Huang and coworkers investigated SERS active core@satellites, Ag nanocube @ Au nanospheres through DNA assisted assembly. Created hot spots from the sharp corners of Ag nanocubes and interfaces between Ag nanocubes and Au nanospheres were asserted by SERS sensitivity to probe molecule, R6G molecules. The obtained core @ satellites are promising for trace amount chemicals and ultrasensitive bio-labeling probes by SERS-based detection.[53]

1.3.1. Synthesis of Noble Metal Nanoparticles

There are many ways to synthesize noble metal nanoparticles in different media, such as chemical, physical, physicochemical and biological. These particles can be generated by two basic approaches; top-down and bottom-up as many other metal nanoparticles.

By using top-down approach, nanoparticles are obtained by decreasing the size of materials from bulk to nano-scale. However, this approach has several drawbacks. One of them is possible defect formation on the surface of nanoparticles. Another one is the requirement of relatively expensive set-ups.[54,55] Moreover, it is very challenging to decrease the size of materials below 100 nm.

Bottom-up approaches are mostly preferred since they provide production of nanoparticles in smaller sizes with more economical set-ups.[55] Bottom-up approach can be performed by following two main ways; *template assisted* and *wet chemical methods.* The *template assisted* one consists of electrochemical, photochemical, electroless processes. The *wet chemical method* comprises chemical reduction, polyol process, hydrothermal process, and seed mediated growth synthesis. Some of these synthesis methods are summarized in the following sections.

8

1.3.1.1. Electrochemical Process

This method was used by Reetz and Helbig for the first time in noble metal nanoparticle generation.[56] To produce size-selective metal nanoparticles, nanoporous membrane templates are employed to deposit the metal ions, which are reduced electrochemically under the applied voltage. Also, surfactant is used as electrolyte and stabilizer is used as template.[57] In the past years, noble metal nanoparticles were synthesized with controlled crystalline properties by applying this method.[58]

1.3.1.2. Chemical Reduction

This method involves reduction of metal salts and this is the basic of all the methods to prepare nanoparticles in various solvents. Au nanoparticles in spherical morphology can be prepared by this method in aqueous medium. The method includes reduction of Au^{3+} ions to Au^0 (in $HAuCl_4$) by sodium citrate in water. Sodium citrate functions as both surfactant and reducing agent. The pioneers of the production of Au nanoparticles (in 10-20 nm size) are Turkevich[59] and Frens[60]. Turkevich first synthesized Au nanoparticles by chemical reduction in 1951 and opened up the way of new synthesis methods.[61] Later, various sizes of Au nanoparticles have been synthesized by wet chemical methods derived from this firstly developed one.[8,62]

1.3.1.3. Hydrothermal Method

Another method for synthesizing the nanomaterials is hydrothermal method in which chemical reaction is performed in solvents contained in closed vessels where the solvents can be heated to around their critical temperature points simultaneously with autogenous pressure. Because the solvent is water, the process is named as *"hydrothermal"*. It is considered as a promising process to prepare both noble metal and other types of nanoparticles. This method provides large amount of nanoparticle

generation with low cost and highly crystalline nanoparticles with desired shape and controllable size. Transition metal nanoparticles, inorganic and metal-organic nanometerials, oxides including group III–V, II–IV, and VI elements are prepared by this method. Also, this process could be utilized for preparing organic nanoparticles without decomposing them at high temperatures and pressures.[63] Metal oxide nanoparticles such as CuO, TiO_2, Fe_2O_3, Al_2O_3, ZrO_2, are synthesized by hydrothermal method.[64,65] The synthesis of noble metal nanoparticles in different morphologies have also been achieved with this method. For instance, Dertli et al. synthesized Au nanowires with high structural purity, aspect ratios and yield by modified hydrothermal method.[66]

1.3.1.4. Seed-mediated method

Seed mediated growth is widely preferred method to prepare noble metal nanoparticles with not only spherical but also anisotropic morphologies, such as nanorods, nanowires and nanostars.[1,31,55,67]

Seed mediated growth method has been developed by Jana et al.[68] It has been modified by "*nuclear method*" of Zsigmondy. This method has several advantages compared to other bottom up methods. Seed and growth process conditions can be adjusted to control the size and shape of the nanoparticles.

This method provides synthesizing various morphologies of Au nanoparticles.[69] Also, specialized equipment is not necessary to produce nanoparticles. The nanoparticles with high yield can be achieved by solution based processing.[70]

This process is made of two step, seed and growth and illustrated in Figure 1.2 which represent the synthesis of Au nanoparticles.[68,71]
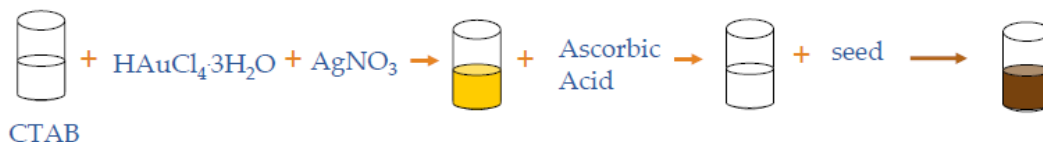
Figure 1.2. The seed mediated growth process of Au nanoparticles

The first seed step comprises production of seed particles by reduction of metal salt by strong reducing agent, usually $NaBH_4$ (sodium borohydride), in the presence of surfactant/capping agent, such as sodium citrate, cetyltrimethyl ammoniumbromide (CTAB)[72] The second step involves the growth of nanoparticles by adding the seed particles to the growth solution containing weak reducing agent, such as ascorbic acid, surfactant (capping agent), like CTAB or polyvinylpropylene (PVP), and shape directing agent, such as $AgNO_3$, and more metal salts.[72] The growth particles are formed by reduction of metal ions with reducing agent on the surface of the seed particles. The concentrations and the kind of reactants used in the growth process have an effect on the size, shape and surface properties.[69] Also, the amount of seed particles have an important role in the size of the synthesized nanoparticles.[55]

The morphologies of nanoparticles are controlled by cooperative action of surfactants and shape directing agents. Surfactant causes a change in the surface energy while controlling the nanoparticle shape.[46] It provides the growth of nanostructures at the specific crystal planes.[73] Nanoparticles with multiple shapes are created by choosing suitable surfactant and particle material, such as nanorods, nanostars, nanocubes and nanowires etc.[46,74]

Goia et al. and Matijevic et al. were studied the production of Au nanoparticles in high yield by using ascorbic acid to reduce Au^{3+} ions to Au^{1+} in the growth step. Particle size and shape have been controlled by the addition of CTAB besides seed particles to the growth solution. In addition, Goia et al. and Jana et al. have generated Au nanospheres with the size between 20 and 100 nm by seed mediated method.[68,75]

The synthesis of Au nanorods by this method starts with generation of seed particles as described above. In the following growth step, obtained seed particles act as nucleation side. Weak reducing agent, ascorbic acid, is employed to reduce more metal salt accompanied with surfactant, CTAB, which control to form the nanorods with determined aspect ratio. It has been investigated that seed mediated growth method is based on the control of the aspect ratio, length divided by width, of the Au nanorods which are controlled by the surfactant, concentration of the seed and reagents.[20,76]

According to research of Murphy et al., seed particles, which was synthesized as citrate stabilized nanospheres, was added to growth solution which includes CTAB, and $AgNO_3$, shape directing agent. $AgNO_3$ not only plays important role in the formation of rod shape with CTAB but also in determination of high yields, crystal structures and optical properties.[77] It was verified that the aspect ratio was adjusted changing the concentration of CTAB and $AgNO_3$.[20] The seed size and concentration are also crucial for the generation of the nanorods with desired aspect ratio.[18,78,79]

Especially, CTAB is extremely important surfactant for production of nanorods with controllable aspect ratio and high yield.[78,80] There are many reported rod synthesis mechanism by using CTAB as surfactant.[20,76,78,81,82,83] Murphy et al. have stated an assumption in which the growth mechanism can correspond to fcc metals and single crystalline seed particles can provide to begin the mechanism. Also, it is promoted the growth of nanoparticles on {111} faces of the nanocrystals, short axis crystal faces, while the binding of the CTAB on {100} faces, long axis crystal faces, and blocking them.[20,71,81,84,85] In other words, the tips of nanorods grow on {111} faces are due to binding the AgBr layers (Br⁻ ions in CTAB) which is formed by $AgNO_3$ and CTAB

to {100} face of nanocrystals.[78] AgBr slows down the reduction of Au and leads to formation of growth of nanorods in a single crystalline form. [77]

The reagents used in nanostar preparation are similar to seed-mediated synthesis of nanorods. After production of seed particles like in nanorod synthesis, ascorbic acid reduces metal salts in the presence of CTAB in the growth step.

Sau et al. observed that the presence of CTAB only causes entirely different Au nanocrystal morphologies. Also, they have an assumption about the following growth mechanism for the evolution of twinned surface spikes. Star formation starts with deposition of Au^0 onto the defect regions of the nearly spherical twinned particles forming small protrusions. The distinct tips are formed on the particle's surface by cooperation of $AgNO_3$ and CTAB.[86]

Yuan and coworkers stated that the presence of Ag^+ ions in media is important to form nanostar. In the absence of Ag^+ ions polydisperse rods and spheres were obtained. It is suggested that the main task of Ag^+ is formation of Ag branches. Also, it assists to grow the Au branches anisotropically on certain crystallographic facets. At the same study, they observed the tips of the stars are usually grown parallel to the {111} twin boundaries roughly along <211> directions.[86,87,88] Ahmed et al. stated that less spiky nanostars are caused by a higher ratio of ascorbic acid:$HAuCl_4$.[89] The preparation of Au seeds provides controlling the size of nanostar. The larger size of nanostars are achieved without seed particles.[87] In contrast, Yuan et al. developed the synthesis of seedless nanostars. These nanostars are biocompatible and have the easy conjugation capability with biomolecules for the next applications.[87]

1.4. Core-Shell Hybrid Systems

Distinctive optical and electronic properties of Au nanoparticles make them attractive materials to do research on and to use in various applications such as catalysis, sensing, optoelectronic devices, photonics, cancer treatment, and drug delivery.[90-93] However, noble metal nanoparticles have poor stability and tend to irreversibly

agglomerate into large particles in harsh environments[9,94,95] due to having high surface energy and van der Waals forces[95], which limit their application areas.[96] The aggregation of nanoparticles causes a broad shift in LSPR band, which hinders the LSPR based sensing applications.[9,97,98] Moreover, the characteristic of surface plasmon absorption is affected by the size and shape of the nanoparticles as well as metal and dielectric surroundings.[8,9] Therefore, it is very important to stabilize them.

Encapsulation of nanoparticles with some coating materials, such as metal oxides,[99] silica and polymeric materials[100] overcomes the agglomeration problem. This kind of coating besides enhancing the stability of metal nanoparticles, controls the dielectric surroundings.[9] Moreover, the optical properties and crystal structures of nanoparticles can be retained even at high temperature treatments.[8]

Metal oxide coatings[7,8,101,102], such as TiO_2, ZnO, MnO_2, Al_2O_3, SnO_2, and silica (SiO_2) contribute to electrical conductivities of nanoparticles and refractive index range. Also, polymer coatings increase their stability and add new functionalities.[9,103,104] The metal core-metal oxide shell structure offers many benefits. They can be summarized as (1) the aggregation of metal nanoparticles can be prevented substantially; (2) metal oxides actualize phase transformation of metal nanoparticles from a liquid phase to a solid phase without abolishing the size dependent properties; (3) metal oxide nanoparticles are deposited as a layer on the surface of metal nanoparticles; (4) metal oxide shells keep protecting both crystal morphology and size of metal nanoparticles at high temperature; (5) they vary refractive indices and dielectric constants.[101,102]

Among all metal core-oxide shell hybrid systems, silica (SiO_2) coating is commonly used due to its relatively easier preparation. Silica coatings present rich surface functionalization, high biocompatibility, controllable porosity and good transparency. Also, they have been widely used to protect the nanoparticles against agglomeration.[7] Mulvaney and coworkers, the pioneer of silica-coated nanoparticles, reported the study on control over thickness of silica coating. They stated that the range of silica thickness and solvent refractive index contribute the control of the optical properties

of the nanostructures.[105] These particles have been used in optoelectronic devices. For example, Zhao et al. studied on improving the performance of organic solar cells by incorporating SiO_2 coated Au nanorods at the interface between active and buffer layer owing to their plasmonic effects.[106] Also, Jankovic et al. demonstrated that the SiO_2 coated Au nanospheres and nanorods into the active layer of an organic photovoltaics device leads to an increase in the photoconversion efficiency (PCE).[107]

Furthermore, silica encapsulated Au nanostars have been employed as substrates to detect probe molecules for highly sensitive SERS-based applications. For example, Chen et al. investigated the $Au@SiO_2$ nanorods and nanoclusters in SERS application as biosensors. They stated that the SERS enhancement is caused by the strong electromagnetic field formed by the plasmon coupling of silica shell on the Au nanoparticles and also LSPR change created by different shape of SiO_2-coated Au nanoparticles. Also, they supported that the applied SERS technique including $Au@SiO_2$ core–shell nanorods and nanoclusters lead to detect the small molecules in trace amounts and they could be used in biosensors.[108]

Atta et al. studied the effects of SiO_2 coated Au nanostars on the surface enhanced Raman scattering (SERS) activity. They observed the increased electric field and enhanced Raman signal dependent on the nanostar morphology and its SiO_2 coating layer.[11] Also, SiO_2 coated Au nanostars were investigated by Fales et al. in SERS-based therapeutic and diagnostic applications. They reported these nanoparticles contribute the singlet oxygen generation.[109]

Although SiO_2 coated Au nanoparticles have been an active research area, a study by Lee et al. revealed the higher stability of SnO_2-coated Au nanoparticles compared to SiO_2-coated ones.[110] The stability comparison of these core-shell structures was performed over a wide pH range. The colloidal nanoparticle solutions were prepared in various pH ranges to observe their behaviors under acidic and basic conditions and monitored over time by visual inspection and collection of extinction spectra. It was determined that the SnO_2-coated Au nanoparticles are more stable than SiO_2-coated Au nanoparticles under basic conditions because of the corruption of the SiO_2 shell at these mediums.[7]

Therefore, tin (IV) oxide has become a promising alternative to widely used silica. It is a convenient material for optical coatings due to being transparent in the visible range. In addition, tin(IV) oxide is an electroconductive material and has consequently been used in the fabrication of transparent electrodes and infrared reflectors.[7,8] Moreover, SnO_2 is a material having great optical and electrical properties, such as high photostability, good carrier mobility[7], high electron mobility[111] and fast electron conductivity.[112] Moreover, it has high thermal and chemical stability, low toxicity and low cost. Because of all these reasons it is an attractive semiconductor material for various applications.

The properties of SnO_2 are similar to the ones of titanium oxide (TiO_2) and zinc oxide (ZnO) as being n-type semiconductor[10,113] with wide band gap (E_g=3.62 eV). They have surface oxygen deficiency, which increase the oxygen vacancies acting as electron donors.[10] SnO_2 is a material widely employed in conventional solar conversion applications. It is doped to obtain a transparent conductor.[7,114]

There are some examples of Au-SnO_2 core-shell structures and their potential uses reported in the literature.[8] This hybrid system is quite attractive since it embodies high potential of enhanced optical, electronic and catalytic performance for various applications[111], such as nanoelectronics and photocatalytic applications.[6,10,115] Chung et al. investigated Au @ SnO_2 core-shell nanoparticles for gaseous formaldehyde sensing application.[116] It has been reported that SnO_2 is an impressive coating material with good gas-sensing property for determination of both oxidative and reductive target gases at the parts per million levels and above.[117] Moreover, the catalytic functions of Au@SnO_2 core-shell nanoparticles for reduction of 4-nitrophenol was investigated by Zhou and coworkers.[9] They reported that SnO_2 shell significantly enhanced the catalytic activity and SnO_2 coated Au nanoparticles have much better catalytic efficiency than uncoated Au nanoparticles.

SnO_2 coatings also contribute to sensing applications. For instance, Jiang and coworkers studied individual Au coated SnO_2 nanowires and 3D branched SnO_2 nanowires encapsulated with Au nanoparticles which were used as SERS substrates.

They reported that these particles provided different SERS enhancement factors. Owing to the large numbers of Au tips and the presence of many hot spots in regions between adjacent Au tips, 3D branched SnO_2 nanowires with Au tips provided higher SERS enhancement factor than the ones with individual Au coated SnO_2.[118] However, to the best of our knowledge the synthesis and potential applications of SnO_2 coated Au nanostars have not been reported, yet.

CHAPTER 2

EXPERIMENTAL

2.1. Chemicals

Hydrogen tetrachloroaurate (III) trihydrate ($HAuCl_4.3H_2O$), L-Ascorbic acid ($C_6H_8O_6$), silver nitrate ($AgNO_3$), sodium stannate trihydrate ($Na_2SnO_3 \cdot 3H_2O$) were supplied from Sigma-Aldrich. Hexadecyltrimethylammoniumbromide (CTAB) was supplied from Fluka. Sodium hydroxide (NaOH), hydrochloric acid (HCl), sodium borohydride ($NaBH_4$), trisodium citrate dihydrate ($C_6H_5Na_3O_7.2H_2O$) were supplied from Merck. All experiments were performed by using deionized water (DI) as solvent having 18.2 MΩ of resistivity.

2.2. Characterization

The SnO_2-coated Au nanoparticles were imaged by using transmission electron microscopy (TEM) and scanning electron microscopy (SEM). Specifically, the characterization of size and morphology of the nanoparticles were done by using JEOL JEM-2100F operating at a voltage of 200 kV for TEM, and FEI Nova Nano SEM 430 for SEM analysis. Energy-dispersive X-ray (EDX) spectroscopy in conjunction with SEM analysis was used to determine the approximate content of Sn, O, and Au of the samples. The absorption spectra were acquired by a Varian model Cary 100 Bio UV-vis spectrophotometer over the wavelength range of 190-1000 nm. X-Ray diffraction (XRD) analysis were performed on a Rigaku D Miniflex pc diffractometer with Cu Kα radiation (λ = 1.54 Å) operating at 30 kV to analyze the SnO_2-coated nanoparticles.

The transmittance spectra of the SnO_2-coated nanoparticles were analyzed by Alpha Bruker model Fourier-Transform Infrared Spectroscopy (FTIR) over the wavenumber 4000-400 cm^{-1}.

The surface enhanced Raman scattering (SERS) signals were achieved by f/9.8, 750 mm spectrometer (Andor SR-750-B1) with 150l/mm grating. The measurements were done by Andor newton^{EM} CCD camera. The source of the Raman excitation was DPSS ND-YAG Laser at 532 nm of wavelength. Nikon Eclipse LV100 microscope was used to focus Halogen 12V50W light source on the substrates. 70 µm diameter of the focal spot size was acquired by 20XA/0.45 objective lens.

2.3. Preparation of Gold Nanoparticles

2.3.1. Preparation of Citrate-Stabilized Gold Nanoparticles

Spherical Au nanoparticles were synthesized by *chemical reduction method.*[8,59] In this method, 0.5 mL of 1% $HAuCl_4.3H_2O$ diluted to 150 mL with DI water in a 250 mL beaker and heated to boiling point while stirring. Then, 10.0 mL of 1.0 wt% $C_6H_5Na_3O_7.2H_2O$ solution was immediately added to the $HAuCl_4$ solution. After about an hour the color of solution turned gradually from light yellow to ruby red. The obtained red color indicates the formation of gold nanospheres.

2.3.2. Preparation of SnO2-Coated Citrate-Stabilized Gold Nanoparticles

For the coating process, the solution including 150 mL of gold nanospheres produced by chemical reduction method was put into 60 °C of water bath. After quick addition of 5.0 mL of 0.04 M sodium stannate trihydrate ($Na_2SnO_3 \cdot 3H_2O$) solution under vigorously stirring, the solution color changed to dark purple. This color change implies that gold nanoparticles are coated with SnO_2 layer. In order to get rid of any impurities and unreacted materials, the obtained colloidal solution were centrifuged at 7000 rpm for 20 minutes and then re-dispersed to 100 mL with DI water.[8]

2.3.3. Preparation of Gold Nanorods

Gold nanorods were synthesized by seed mediated growth method.[3] Firstly, the seed solution was prepared and obtained gold seed nanoparticles. In the following step, the growth solution was prepared to obtain rod shaped nanoparticles.

Seed solution was prepared by mixing 1.25 mL of 0.002 M $HAuCl_4.3H_2O$ solution with 2.74 mL of DI water. Then, 3.76 mL of CTAB was added to the solution. After the addition of 0.90 mL of 0.01 M freshly prepared ice-cold $NaBH_4$, the color of solution changed from dark yellow to light brown and the solution was vigorously stirred for 2 minutes. Finally, obtained solution was hold undisturbed at 27 °C for 2 hours.

Growth solution was prepared by adding 0.4 mL of 0.01 M $HAuCl_4.3H_2O$ solution to 4.15 mL of DI water. An orange colored solution was obtained by first adding 4.75 mL of 0.2 M CTAB and then 0.06 mL of 0.01 M $AgNO_3$ solution. After the addition of 0.64 mL of 0.01 M ascorbic acid, the solution becomes colorless. Finally, 31.30 μL of prepared seed solution was added to the growth solution by gentle mixing and kept undisturbed inside 27 °C water bath for 24 hours.

2.3.4. Preparation of SnO_2-Coated Gold Nanorods

Au core-SnO_2 shell nanorods were performed by hydrothermal-based method as described in literature.[9] Firstly, 5.0 mL of gold nanorod solution was diluted to 20 mL with DI water. 0.1 M of NaOH solution was added drop by drop to adjust the pH of the solution to 10.5 while stirring. Then, the solution was placed into a 75 °C of oil bath. After vigorous stirring for 15 minutes, 3.0 mL of aqueous solution of 4.0 mM $Na_2SnO_3.3H_2O$ was added to this solution and stirred for two more hours. Finally, the solution was centrifuged at 7000 rpm for 20 minutes and re-dispersed to 5.0 mL with DI water.[9]

2.3.5. Preparation of Gold Nanostars

Star shaped gold nanoparticles were synthesized by seed mediated growth method.[11] 15 nm citrate stabilized Au seed solution was prepared by Turkevich method as described above. Then, 40 μL of 1.0 M HCl and 2.5 μL of Au seed solution were added to 10.0 mL of 0.01 M M $HAuCl_4.3H_2O$ solution in a 20.0 mL of glass vial by stirring gently at 700 rpm. 400 μL of 0.003 M $AgNO_3$ and 200 μL of 0.1 M ascorbic acid solution were mixed with this solution simultaneously. After rapid addition of 2.0 mL of 0.2 M CTAB solution, the growth solution was stirred for another 30 minutes. At the end of stirring, the gold nanostars were produced. Finally, the solution was centrifuged at 3200 rpm for 25 minutes and the particles were dispersed to 10.0 mL DI water.

2.3.6. Preparation of SnO_2-coated Gold Nanostars

A procedure, which was previously reported to produce SnO_2-coated Au nanorods[9], was modified to coat the gold nanostars with SnO_2 layer. In this process, firstly 20 mL of aqueous solution was prepared by diluting 5.0 mL of CTAB stabilized Au nanostars with DI water. 0.1 M of NaOH solution was used to adjust pH of the solution to 10.5. The solution was vigorously stirred in 75 ºC oil bath. After 15 minutes, 3.0 mL of 40 mM $Na_2SnO_3.3H_2O$ aqueous solution was added to the solution and stirred for another 2 hours. Finally, the centrifugation of coated Au nanostars was done at 3200 rpm for 25 minutes and they were re-dispersed in 5.0 mL DI water.
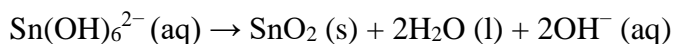
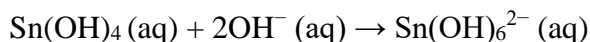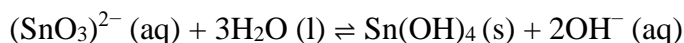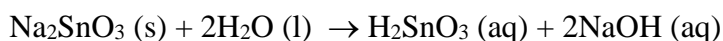### 2.4. Preparation of SERS Samples

Samples including the mixture of gold nanostars and crystal violet (CV) solution were added on Si wafer by drop-casting method for SERS application. The Raman signals were measured from 5 different regions of the samples. Firstly, uncoated gold

nanostars and SnO_2-coated gold nanostars were mixed with crystal violet (CV) solutions of different concentrations (10^{-4} M, 10^{-5} M, 10^{-6} M) in 5:2 ratio of Au nanostar:CV. Prepared mixtures were then dropped onto the Si wafer. The samples were air-dried before Raman analysis.

CHAPTER 3

RESULTS AND DISCUSSION

SnO$_2$ coated Au nanoparticles in star, rod and spherical morphology were synthesized by an one-step hydrothermal-based method similar to the ones reported in the literature.[119] The method involves mixing Au nanoparticles with Na$_2$SnO$_3$ precursor in alkaline aqueous medium and formation of SnO$_2$ shell on Au nanoparticle core. In this process, Na$_2$SnO$_3$ rapidly hydrolyze and then oxidize to form SnO$_2$ according to proposed chemical reactions given below:[120]

$$Na_2SnO_3 \text{ (s)} + 2H_2O \text{ (l)} \rightarrow H_2SnO_3 \text{ (aq)} + 2NaOH \text{ (aq)}$$

$$(SnO_3)^{2-} \text{ (aq)} + 3H_2O \text{ (l)} \rightleftharpoons Sn(OH)_4 \text{ (s)} + 2OH^- \text{ (aq)}$$

$$Sn(OH)_4 \text{ (aq)} + 2OH^- \text{ (aq)} \rightarrow Sn(OH)_6^{2-} \text{ (aq)}$$

$$Sn(OH)_6^{2-} \text{ (aq)} \rightarrow SnO_2 \text{ (s)} + 2H_2O \text{ (l)} + 2OH^- \text{ (aq)}$$

Finally, the SnO$_2$ starts to deposit on the Au nanoparticles and act as a nucleation site for the growth of SnO$_2$ layer on their surface. The characterization of synthesized SnO$_2$ coated star, spherical and rod-shaped Au nanoparticle systems as well as the SERS investigation on Au nanostar-SnO$_2$ core-shell system are discussed in the following sections.

3.1. Characterization of SnO$_2$ coated Au nanostars

TEM and SEM micrographs show that SnO$_2$ coated gold nanostars have average size of ca 400 nm±100 nm. (Figure 3.1). These nanoparticles have three-dimensional structures with various numbers of tips growing out of the nanoparticle core.

TEM analyses clearly show existence of a layer on Au nanostars with ca. 20±5 nm thickness. (Figure 3.2). EDX analysis provided primitive information on elemental character of this layer. The data acquired from different parts of the core-shell nanoparticle system shows strong signals of gold and relatively weaker signals of Sn. (Figure 3.1e). This observation suggests the formation of a layer of SnO_2 on the nanoparticle surface.
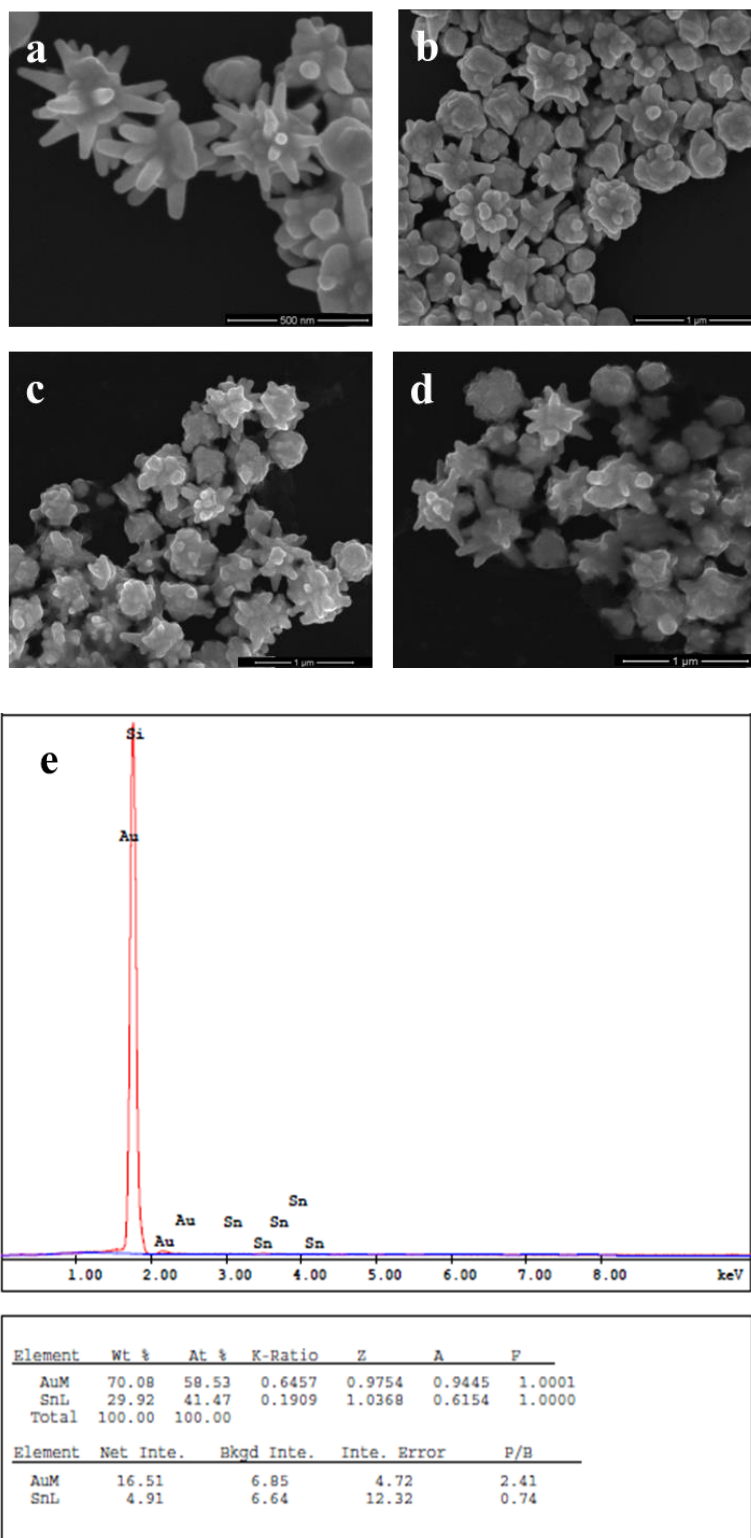
Figure 3.1. SEM images of **(a,b)** non-coated and **(c,d)** SnO$_2$ coated Au nanostars. **(e)** EDX spectrum of SnO$_2$-coated Au nanostars.
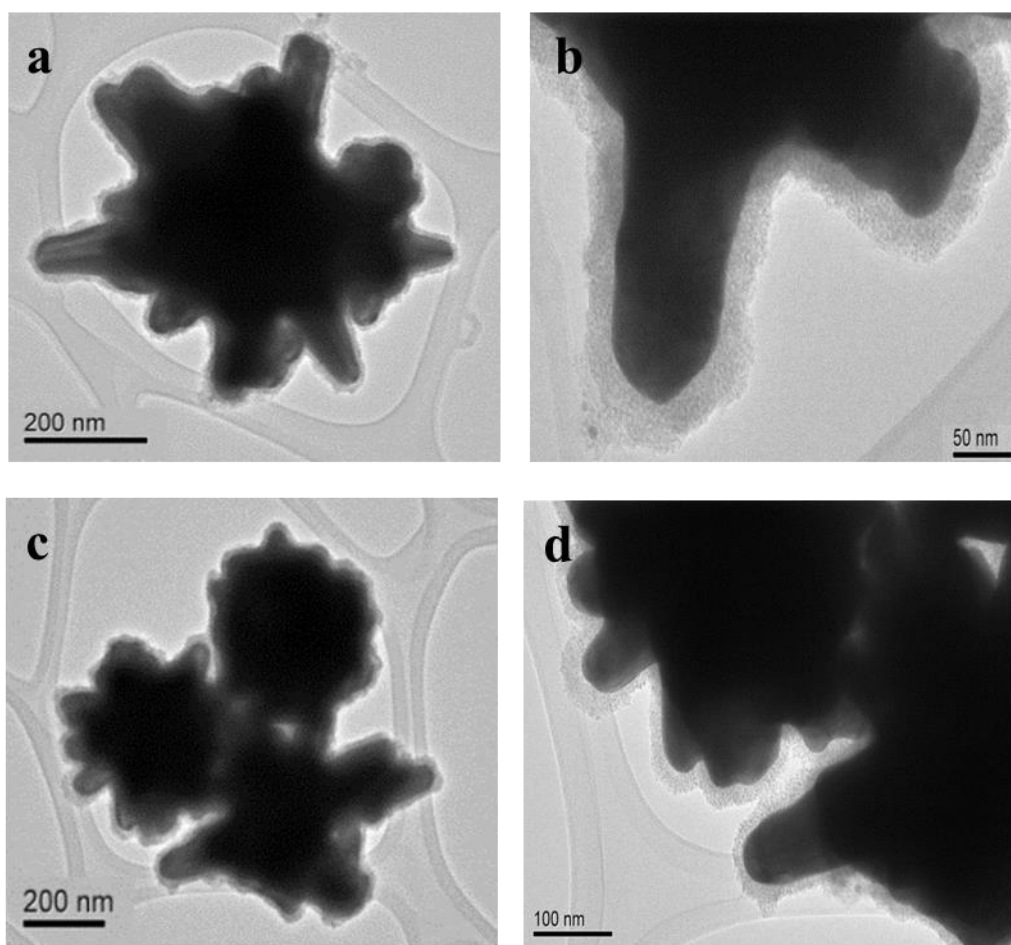
Figure 3.2. TEM images of SnO$_2$ coated Au nanostars.

Figure 3.3 shows UV-vis absorption spectrum of the SnO$_2$-coated and non-coated Au nanostars. Both spectra has very broad plasmon band with maximum intensity around 605 nm. The broadness of the bands is most likely due to the structural diversity of Au nanostars. The color of the nanoparticle solution changed from dark blue to greenish-blue upon SnO$_2$ coating. UV-vis analyses provided to observe the change in the particles' optical properties. The absorption spectrum shows a decrease in plasmon band intensity as well as a slight broadening toward higher wavelengths upon SnO$_2$ coating. Decrease in intensity could be because of the existence of a layer on Au

nanostars and/or changes in the concentration in nanoparticle solution during purification processes. Broadening and very slight red-shift in the band are most likely due to change in the structural and surface characteristics of gold nanoparticles with SnO_2 coating. This observation is consistent with the ones previously reported in the literature.[8,9]
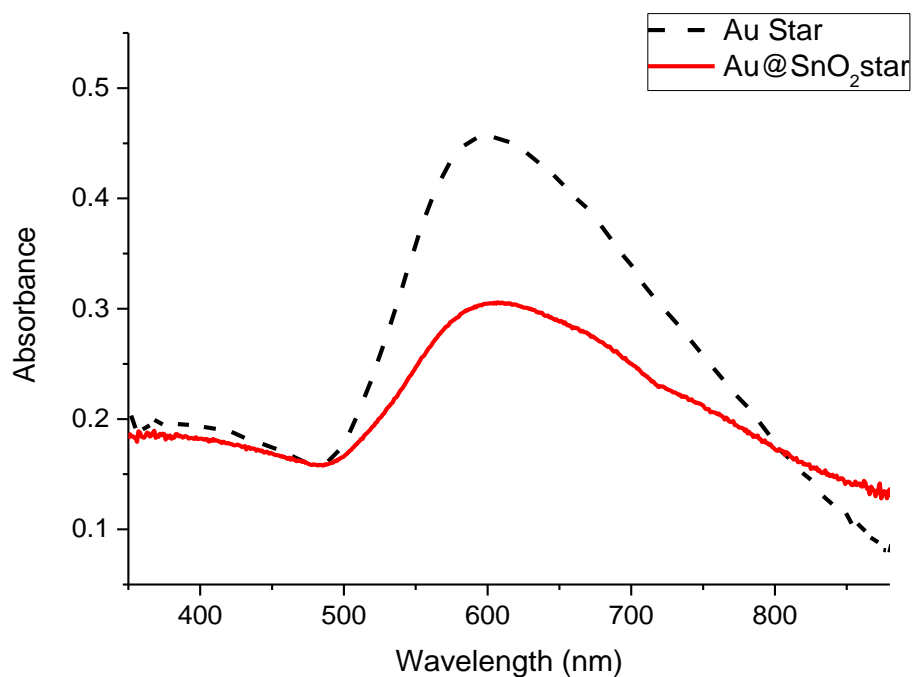

Figure 3.3. UV-vis spectra of SnO_2 coated and non-coated Au nanostars.

XRD pattern was performed to characterize the identity and crystalline nature of the layer on gold nanostars. (Figure 3.4). The analysis verifies the presence of both Au and SnO_2 in the synthesized hybrid system. The peaks of Au nanoparticles with face centered cubic (fcc) were observed at 2Θ: 38.33°, 44.40°, 64.72°, 77.74°, 81.84°, and they are indexed to (111), (200), (220), (311), (222) planes, respectively. (JCPDS: Card No. 04-0784)[9] . The diffraction peaks at 2Θ: 26.43°, 34.11° and 52.09° are

assigned to (110), (101) and (211) lattice planes of SnO_2 with rutile structure, respectively (JCPDS: Card No. 77-0451).[9] The intensities of SnO_2 diffraction peaks are significantly lower relative to the ones of gold. This is most likely due to the presence of very low amount of SnO_2 on the shell compared to the amount of Au in nanostar core.
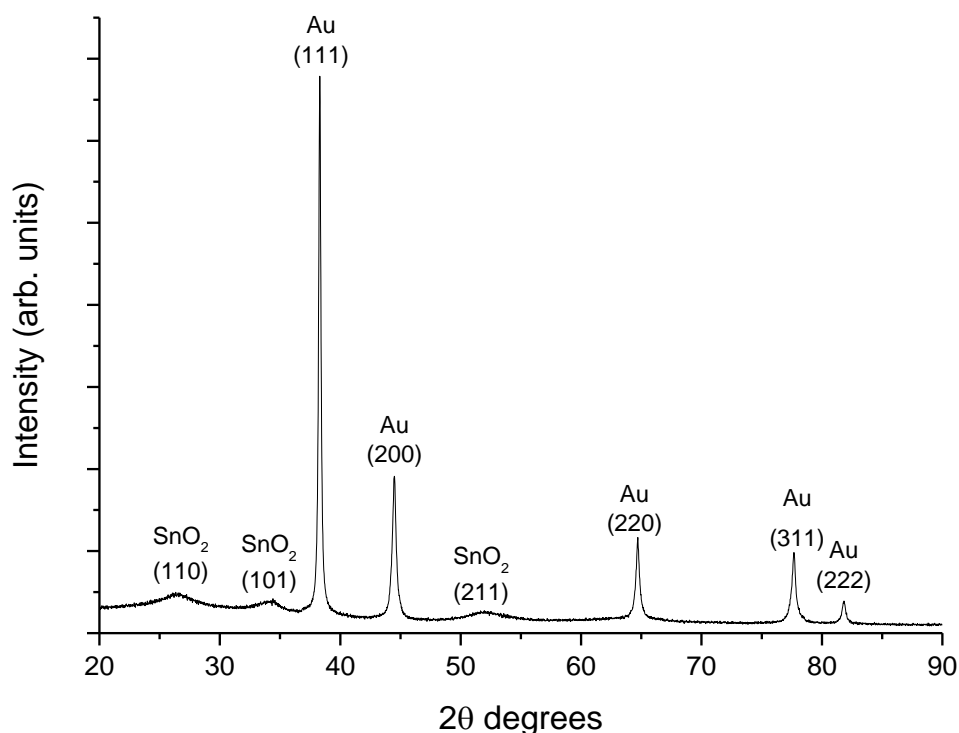

Figure 3.4. XRD pattern of as-prepared SnO_2 coated Au nanostars
(JCPDS Card No. 01-089-4898)

The FTIR analysis was also employed to verify the presence of SnO_2 layer on the gold nanostars. Figure 3.5 shows the FTIR spectrum of as prepared SnO_2 coated gold nanostars. The bands at 940 and 581 cm^{-1} were assigned to the Sn-O and O-Sn-O stretching modes of SnO_2, respectively.[121] The peaks at 3447 cm^{-1}, 1636 cm^{-1} and 1214 cm^{-1} were assigned to O-H stretching vibration of water molecules as the

spectrum was collected in aqueous medium.[121,122] Bending modes of H-O-H of the water are observed at 1463 cm^{-1}.[121] The peaks at 2917 cm^{-1} and 2853 cm^{-1} were assigned to C-H band of CTAB molecule which represents the vibrations of CH$_3$-N bounds in CTAB molecule.[123]
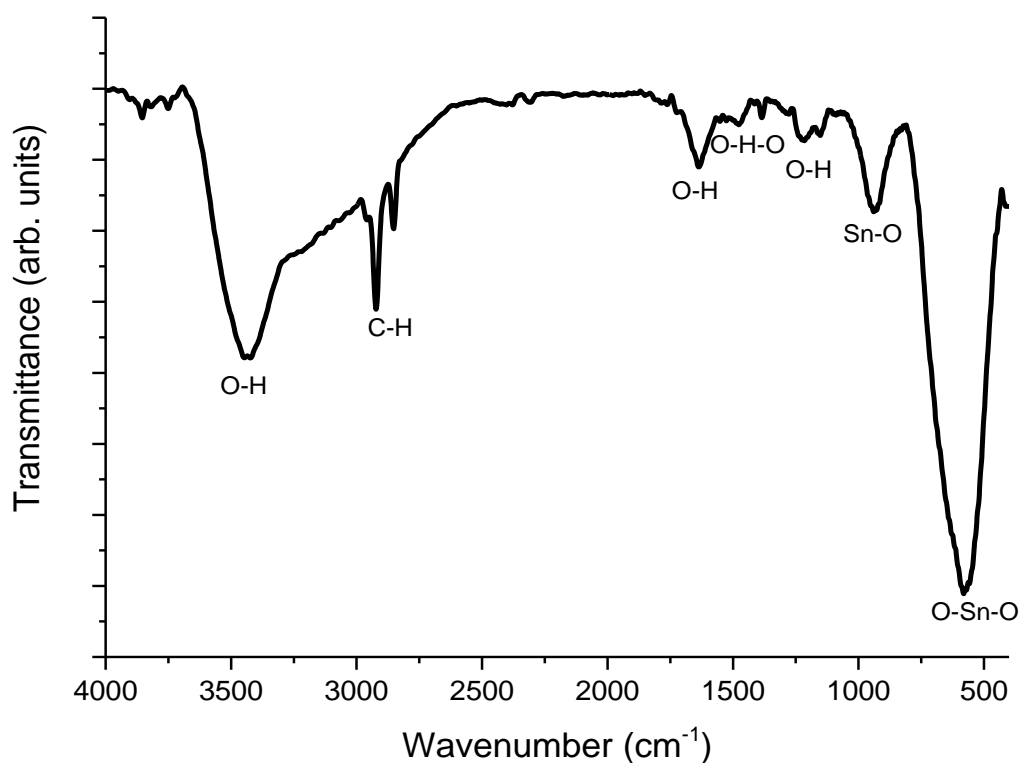
Figure 3.5. FTIR spectrum of SnO$_2$ coated Au nanostars.

3.2. Characterization of SnO$_2$ coated Au nanospheres

TEM and SEM micrographs of Au nanospheres before and after SnO$_2$ coating are shown in Figure 3.6. TEM images clearly show the formation of core-shell structure of the synthesized hybrid system. The average diameter of the Au nanosphere core is

about 15 ± 5 nm while the thickness of the tin oxide shell is ca. 20 ± 5 nm. Thus, the overall size of the hybrid system is measured as ca. 55 ± 10 nm. EDX spectrum is demonstrated in Figure 3.6 c. On the contrary to the EDX spectrum of SnO_2-coated nanostars and nanorods, the one of Au nanosphere-SnO_2 system shows significantly stronger signals of Sn compared to the Au signals. This is because of the presence of notably larger amount of SnO_2 on the shell compared to the amount of Au in hybrid nanoparticles' core.
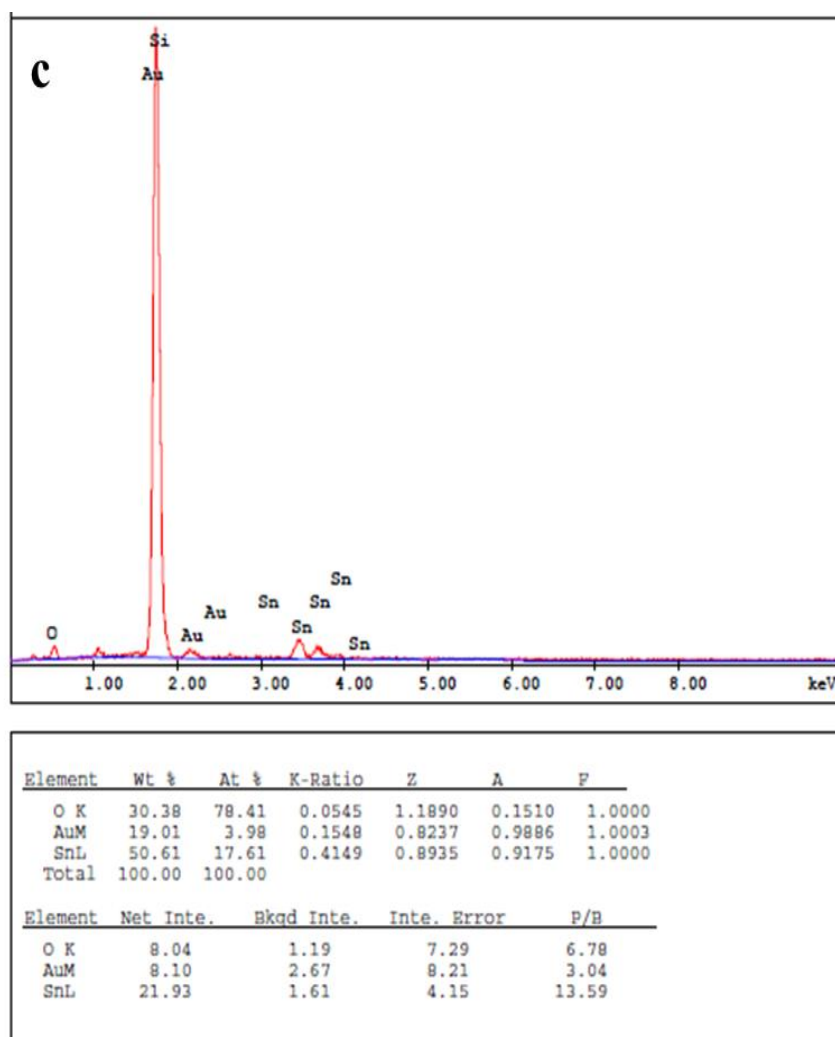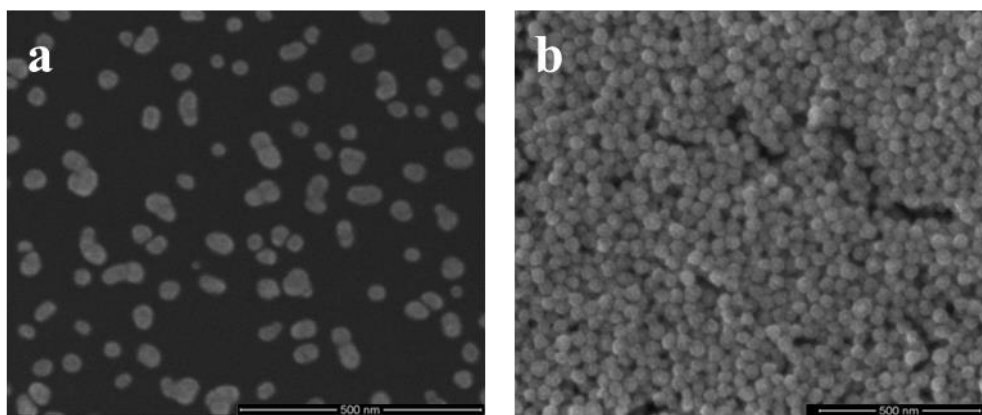
Element	Wt %	At %	K-Ratio	Z	A	F
O K	30.38	78.41	0.0545	1.1890	0.1510	1.0000
AuM	19.01	3.98	0.1548	0.8237	0.9886	1.0003
SnL	50.61	17.61	0.4149	0.8935	0.9175	1.0000
Total	100.00	100.00				

Element	Net Inte.	Bkgd Inte.	Inte. Error	P/B
O K	8.04	1.19	7.29	6.78
AuM	8.10	2.67	8.21	3.04
SnL	21.93	1.61	4.15	13.59

Figure 3.6. SEM images of **(a)** non-coated **(b)** SnO₂ coated Au nanospheres **(c)** EDX spectrum of SnO₂ coated Au nanospheres.
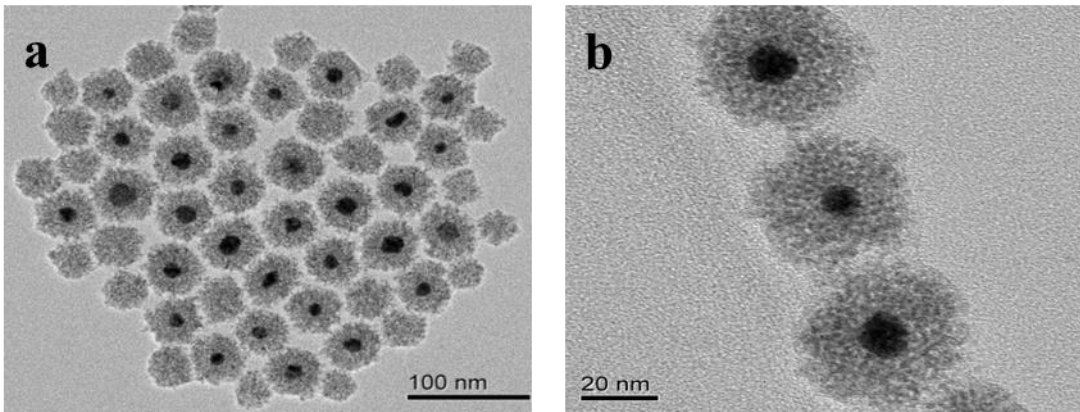
Figure 3.7. TEM images of SnO$_2$ coated Au nanospheres.

Figure 3.8 demonstrates UV-vis absorption spectra of the SnO$_2$ coated and non-coated Au nanospheres. The spectra show that plasmon band of non-coated Au nanospheres at 523 nm is red-shifted to 542 nm after SnO$_2$ coating, as expected. Similar to the Au nanostars, here too, the change in surface characteristics resulted in changes in optical properties of these nanoparticles. After the nanoparticles are coated, the medium changes from water to SnO$_2$. Because the refractive index of the surrounding medium increases, strong red shift of surface plasmon peaks is observed in the visible range of light. This change is monitored by UV-vis spectroscopy.[10,124] *(refractive indeces n$_{water}$ = 1.33 and n$_{SnO2}$ = 2.0)*[10]
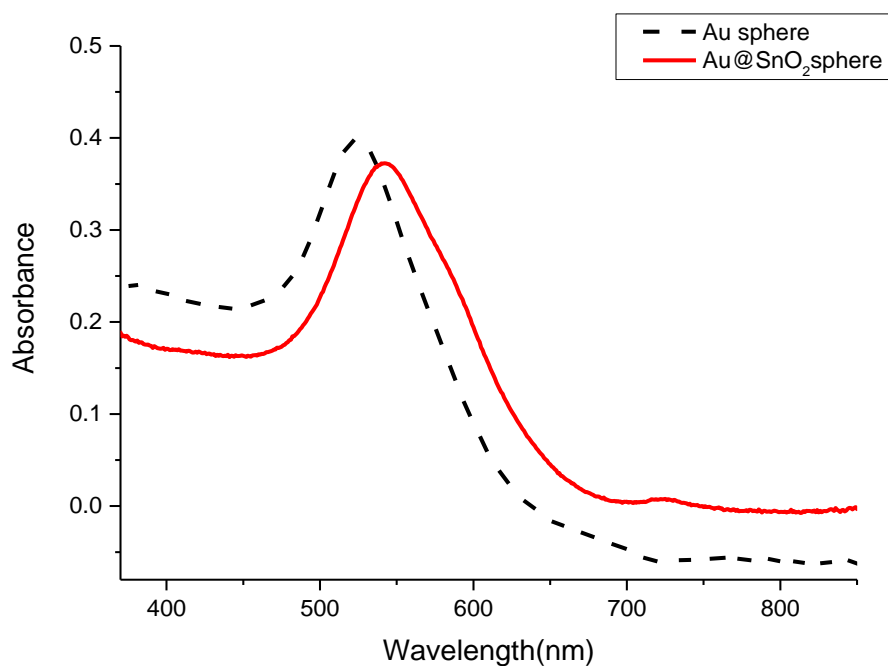
Figure 3.8. UV-vis spectra of before and after SnO_2 coating.

XRD pattern was performed to verify the formation of SnO_2 layer on Au nanospheres. Figure 3.9 illustrates XRD pattern of SnO_2 coated Au nanospheres. Similar to the SnO_2 coated nanostars, the peaks at 2Θ: 38.21º, 44.64º, 64,98º, 77.74º and 81.73º are assigned to the (111), (200), (220), (311) and (222) lattice planes of Au with fcc structure. The peaks that correspond to (110), (101) and (211) planes of SnO_2 with rutile structure are observed at 2Θ: 26.29º, 33.99º and 51.72º.
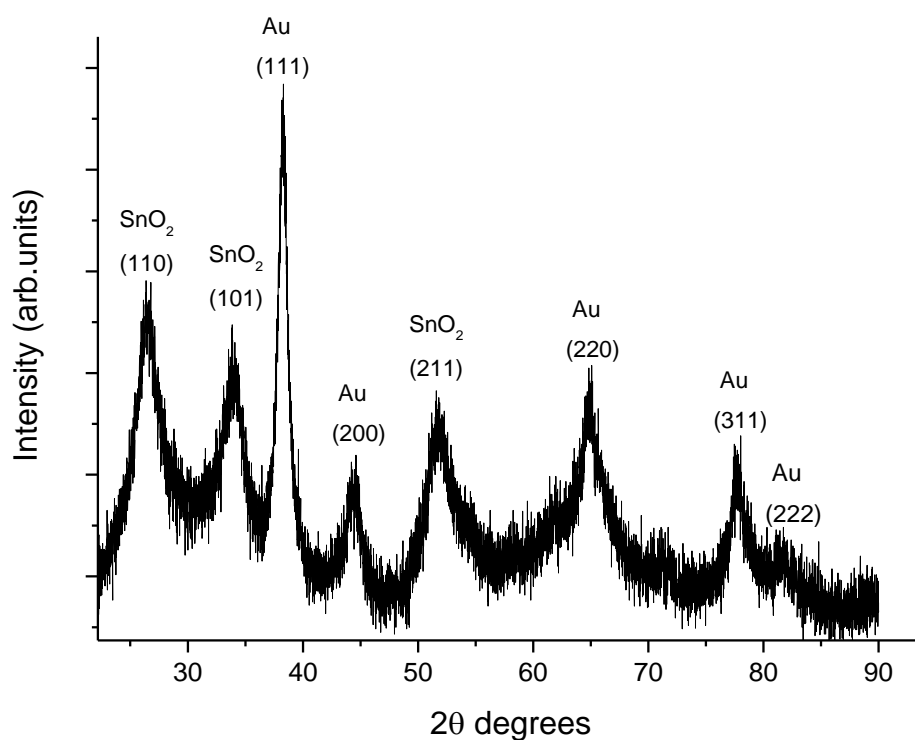
Figure 3.9. XRD pattern of as-prepared SnO_2 coated Au nanospheres (JCPDS Card No. 04-0784 and 77-0451 for Au and SnO_2, respectively.)[8]

Figure 3.10 shows the FTIR spectrum of SnO_2 coated gold nanospheres. The bands at 947 and 584 cm^{-1} are assigned to stretching modes of O-Sn-O and Sn-O.[121] The peaks at 3418 and 1634 cm^{-1} demonstrated the presence of O-H bonds belonging to the adsorbed water molecule.[121,122] The bands at 1380 cm^{-1} was assigned as bending modes of H-O-H of water molecule.[121]
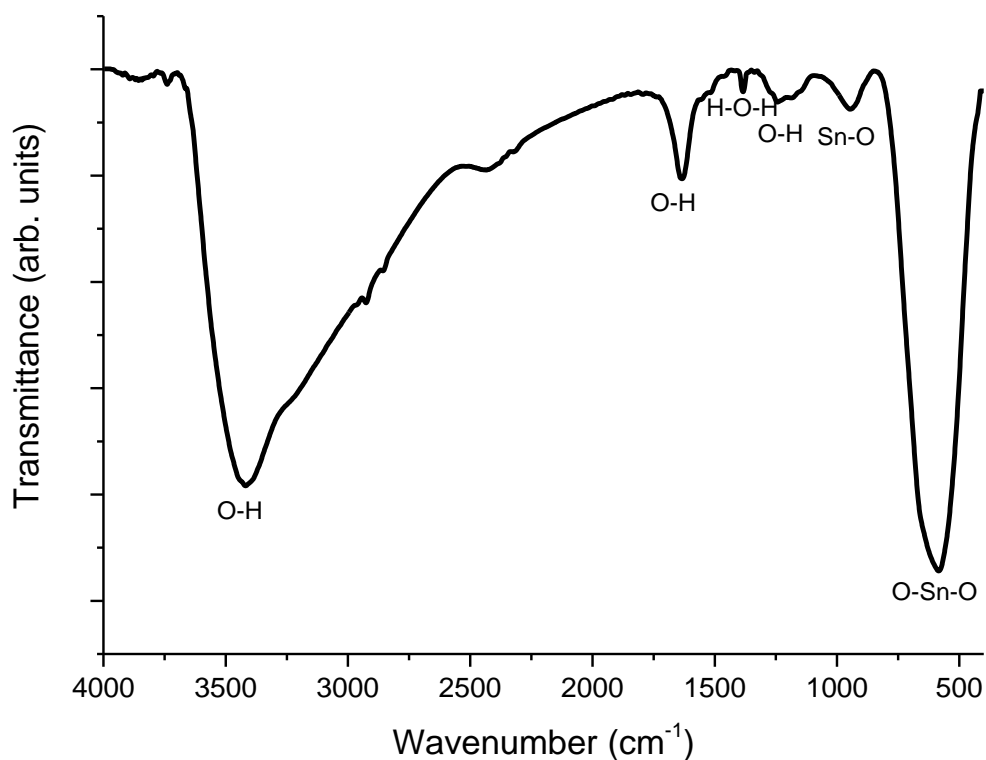
Figure 3.10. FTIR spectrum of SnO_2 coated Au nanospheres.

3.3. Characterization of SnO_2 coated Au nanorods

SEM and TEM analyses were performed to observe possible changes in nanoparticle morphology before and after coating them with SnO_2. TEM and SEM images show that the average length of the gold nanorods is 58 ± 10 nm with an average diameter of 12 ± 5 nm. (Figure 3.11). After the coating process, a shell with a thickness of ca. 10 ± 5 nm formed on the nanoparticles. (Figure 3.12). The analyses also show that the formation of a layer does not result in any change on the morphology of the nanoparticle core. The coating on the gold nanorods was also characterized by EDX analysis. The EDX spectrum shows the signals of gold and tin, suggesting the existence of SnO_2 layer on the gold nanorods. (Figure 3.11e).
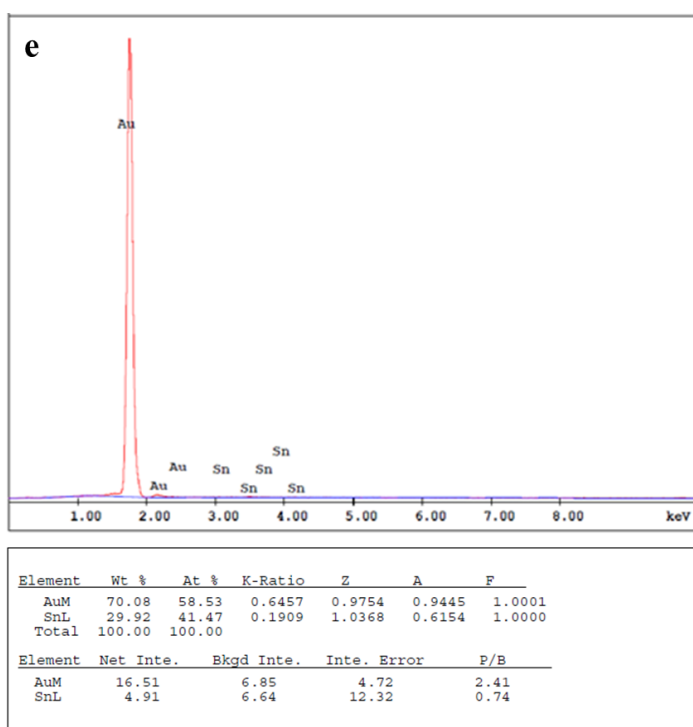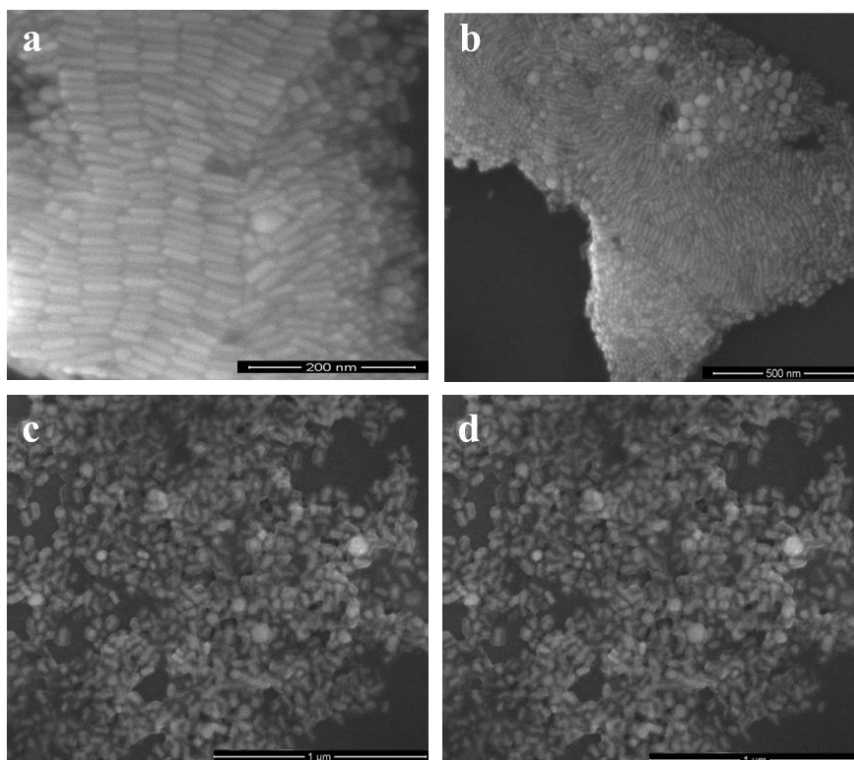
Figure 3.11. SEM images of **(a,b)** non-coated, **(c,d)** SnO$_2$ coated Au nanorods.**(e)** EDX spectrum of SnO$_2$ coated Au nanorods.
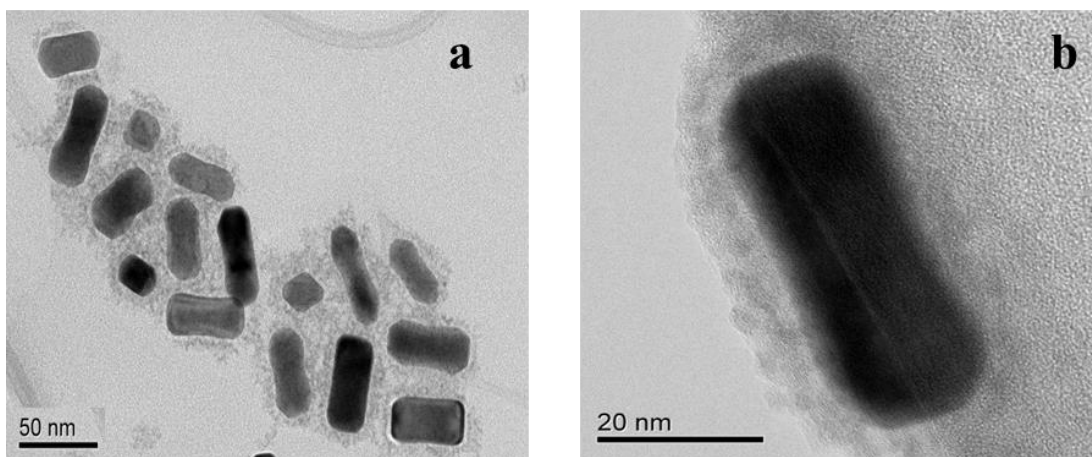
Figure 3.12. TEM images of SnO$_2$ coated Au nanorods.

Figure 3.13 shows the UV-vis spectra of SnO$_2$ coated and non-coated gold nanorods. The spectra illustrate two characteristic absoption bands; longitudinal and trasverse bands, of gold nanorods at 516 nm and 696 nm, respectively. While the longitudinal band results from absorption of the light through long axis of nanorods, the transverse bands represent the optical properties of short axis of the rods.[125] The spectrum shows that the SnO$_2$ coating on Au nanorods leads to shift of the absorption bands. The observed red-shift is more significant for the longitudinal band (shifted to 715 nm). The variations in the surface characteristics lead to changes in optical properties of the nanorods, as expected. These changes have higher impact on longitudinal band and observed more clearly as previously reported in literature.[9] Moreover, the most likely reason for the red-shift of bands is high refractive index of the coating material.[8,9,10]

Figure 3.13. UV-vis spectra SnO_2 coated and non-coated Au nanorods.
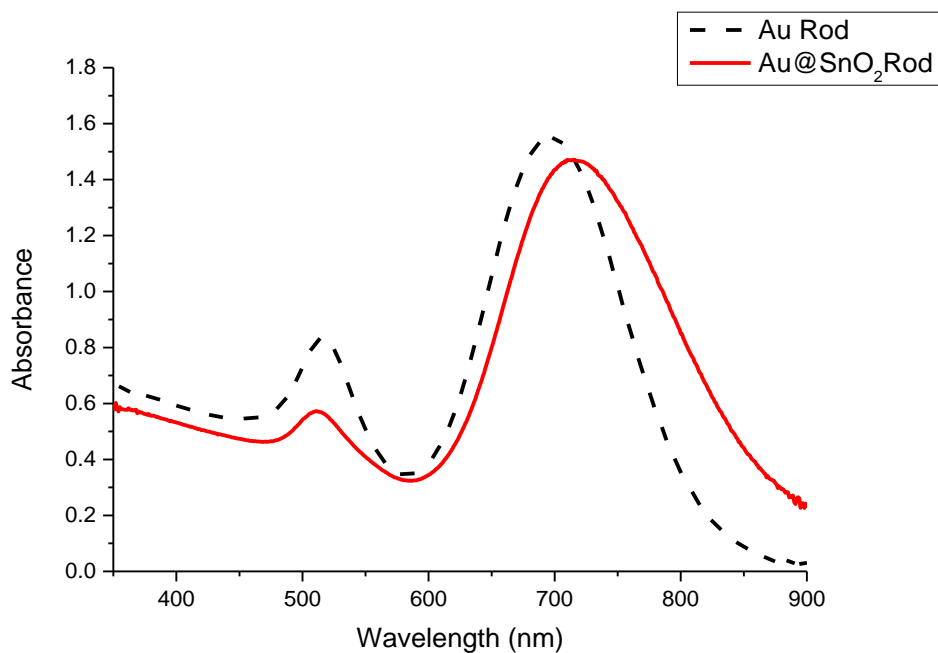
Figure 3.14 demonstrates XRD pattern of SnO_2 coated gold nanorods. The diffraction peaks at 2Θ: 38.33°, 44.52°, 64.72°, 77.74° and 81.96° were indexed to (111), (200), (220), (311) and (222) lattice planes of fcc structure of Au nanoparticles. The peaks that correspond to (110) and (101) planes of SnO_2 are barely observed at 2Θ: 23.33° and 31.64°.[126]
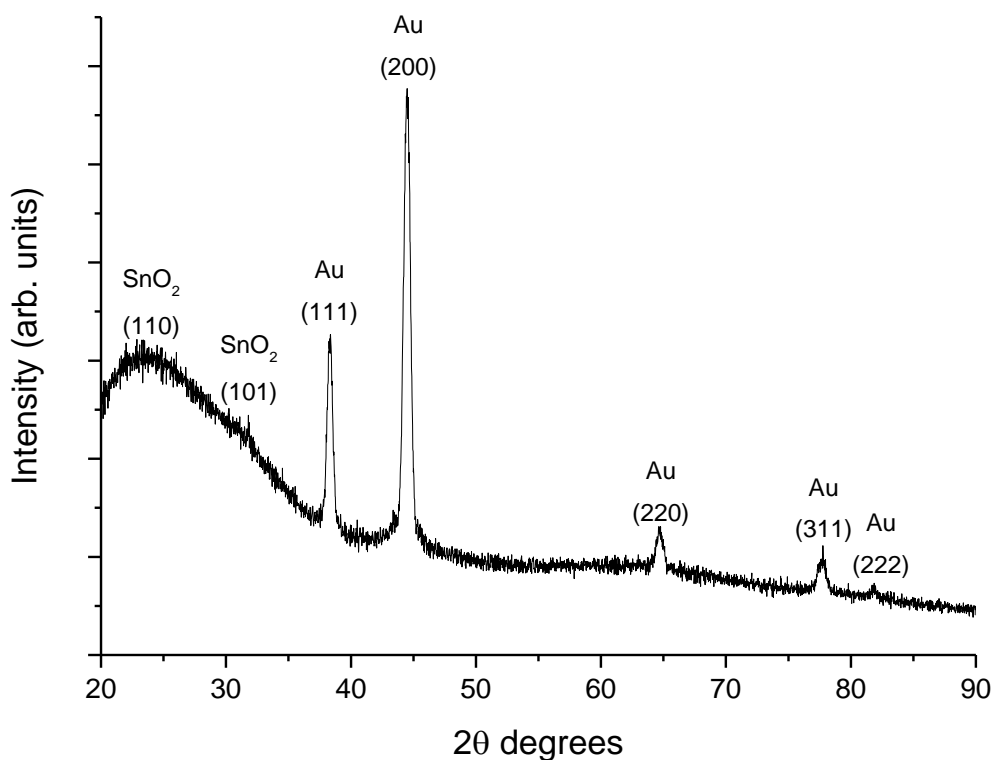
Figure 3.14. XRD pattern of as-prepared SnO_2 coated Au nanorods (JCPDS Card No. 01-089-4898)

Figure 3.15 shows the FTIR spectrum of SnO_2 coated Au nanorods. Similar to the one of SnO_2-Au nanostars, here too, the SnO_2 bands are observed at 570 and 941 cm^{-1}.[121] The peaks at 3408 cm^{-1}, 1628 cm^{-1} and 1221 cm^{-1} indicated the presence of O-H bonds belonging to the adsorbed water molecule.[121,122] The C-H bands of CTAB molecule which displays the vibration in CH_3-N group of CTAB molecule were illustrated at 2923 cm^{-1} and 2847 cm^{-1}.[123]

Figure 3.15. FTIR spectrum of SnO_2 coated Au nanorods

3.4. Surface-enhanced Raman scattering properties of SnO_2 coated Au nanostars

Among all nanoparticle morphologies studied, star-shaped ones have superior optical properties. This mostly originate from their anisotropic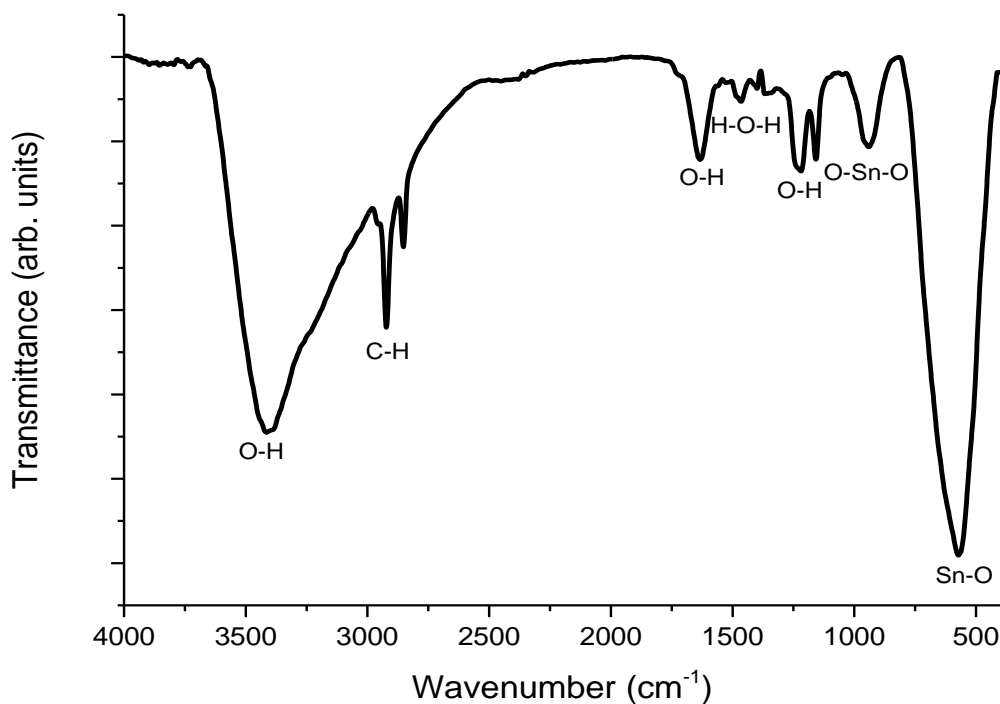 morphologies with sharper features compared to spherical and rod-shaped nanoparticles. These features lead Au nanostars to be better substrates for SERS applications. The significantly higher SERS activity of Au nanostars compared to nanospheres and nanorods have been reported previously by Esenturk et al.[1] Therefore, SERS property of only SnO_2 coated Au nanostars have been investigated in this thesis study. SERS activity of SnO_2 coated Au nanostars as well as non-coated Au nanostars were studied by using crystal violet (CV) as a probe molecule. Figure 3.16 shows SER spectra of CVadsorbed on Au nanostars. The number of vibrational modes detected and their relative intensities were

42

reproducible for all the batches of nanoparticles. The SER spectra show that all of the vibrational modes of CV are observed clearly before and after SnO_2 coating. The observed vibrational modes of CV molecule are in good agreement with the ones reported in the literature.[127,128] These CV modes can be classified in three main groups. The first group associate with the central carbon atom (C^+-phenyl vibrations), and they appear below 450 cm^{-1}. The second group of vibrations involve nitrogen atoms (N-phenyl stretching), and they are observed between 1350 cm^{-1} and 1400 cm^{-1}. Finally, the modes of phenyl rings appear between 400 cm^{-1} and 1300 cm^{-1} (for skeletal ring vibrations and ring C–H deformations), and above 1400 cm^{-1} (for ring stretching modes). The enhancement and possible shift in peaks were observed by using CV vibrational modes of C^+-phenyl bending at 345 cm^{-1}, ring C–H bending at 805 and 1175 cm^{-1}, ring skeletal vibration of radical orientation at 920 m^{-1}, N-phenyl stretching at 1371 cm^{-1}, and ring C–C stretching at 1581 cm^{-1} and 1616 cm^{-1}. Figure 3.16a demonstrates the comparison of SER spectra of gold nanostars before and after SnO_2 coating, raw Raman spectra of CV and nanostars without adding CV. The Raman spectra of nanostars do not show any signal that would prevent the observation of CV modes. Enhancements of all the CV modes are observed when the molecule adsorbed both on SnO_2 coated and non-coated Au nanostars. On the other hand, Raman spectra of CV with 10^{-4} M concentration show signals of only a few modes of the molecule. In addition, a decrease in the intensities of SERS signals after the SnO_2 coating on Au nanostars as expected. This is mostly because of the presence of SnO_2 coating, which can both decrease electromagnetic enhancement effect of nanostars, and increase the distance between the Au nanoparticle surface and CV molecule.

The enhancement factor (EF) calculations for SnO_2 coated Au nanostars would not yield very accurate results since the studied nanoparticle system has irregular, three-dimensional morphology as well as nonuniform SnO_2 coating. Hence, the calculation was performed only to estimate a rough lower limit EF for Au nanostar-SnO_2 system. The following equation was used for EF calculations;[38,129,130]

$$EF = (I_{SERS}/I_{Raman}) \text{ x } (N_{Raman}/N_{SERS})$$

I_{SERS} and I_{Raman} represent the intensities of a vibrational mode of the probe molecule observed in SERS and Raman, respectively. N_{SERS} and N_{Raman} are the number of analyte molecules excited under the laser spot in bulk sample and adsorbed on Au nanoparticles, respectively. The CV mode at 1616 cm^{-1} was used to determine I_{SERS} and I_{Raman} of the molecule. The details of the N_{SERS} and N_{Raman} calculations are given in Appendix. It is essential to specify that the N_{SERS} calculations was done by assuming studied nanoparticles having spherical structures with average sizes of 400 nm. This assumption was made because of the difficulties associate with nonuniform structure, thus not well-defined surface areas star shaped Au nanoparticles as stated above.

The EFs were estimated as $2.51 \times 10^6 \pm 0.51 \times 10^6$ for non-coated Au nanostars and $2.25 \times 10^6 \pm 0.40 \times 10^6$ for SnO$_2$ coated Au nanostars. In these calculations, all the added CV molecules are assumed to adsorb on nanoparticles' surface and all of them equally contribute to the detected SERS signal intensity. Because of these, the estimated EFs show only the lower limit values and both coated and non-coated Au nanostars are expected to yield higher EF values.

Alternative way to assess SERS performances of synthesized nanoparticle systems is to determine their detection limits. The detection limit represents minimum concentration of the probe molecule that can be detected on the studied nanoparticles. Figure 3.16 b shows that vibrational modes of the CV strongly enhance 10^{-4} M, 10^{-5} M and 10^{-6} M CV concentration when the molecule adsorbed on SnO$_2$ coated Au nanostars. The further decrease in the concentration leads to significant decrease in the SERS signal intensity and the modes are barely detected below 10^{-6} M of CV concentration.
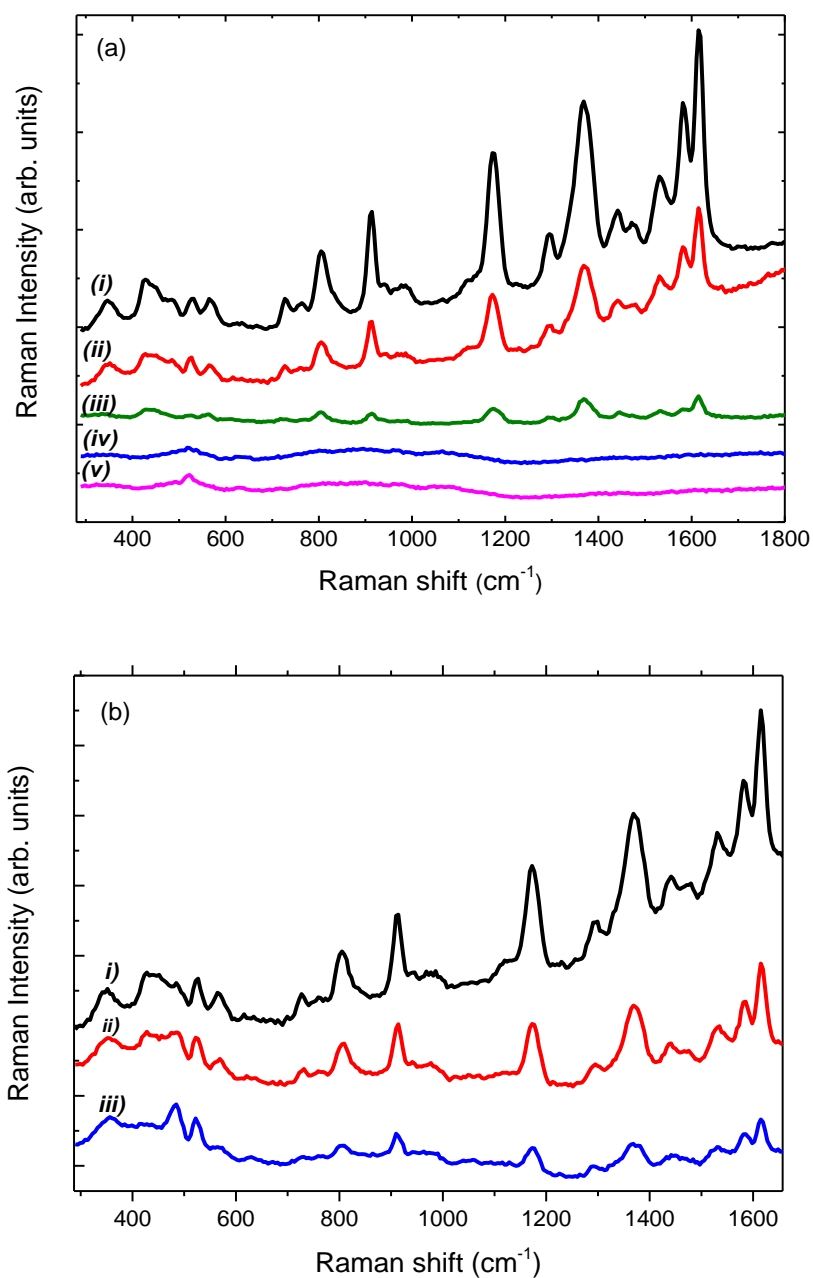
Figure 3.16. (a) SER spectra of 10^{-4} M CV on *(i)* non-coated and *(ii)* SnO$_2$-coated Au nanostars. Raman spectra of *(iii)* 10^{-4} M CV, (iv) non-coated Au nanostars (before CV addition) and *(v)* SnO$_2$-coated Au nanostars (before CV addition). **(b)** SER spectra of *(i)* 10^{-4} M CV, *(ii)* 10^{-5} M CV and *(iii)* 10^{-6} M CV on SnO$_2$-coated Au nanostars.

CHAPTER 4

CONCLUSION

Gold nanoparticles, in particular the ones with anisotropic morphologies, have become focus of intense research due to their remarkable properties, which make them promising materials in chemical, biomedical, sensing, imaging and solar cells applications. Stabilizing these nanoparticles is very crucial for their potential applications. One way to achieve this is to coat them with appropriate materials that preserve their unique properties.

In this study, the star-shaped gold nanoparticles were encapsulated with optically transparent SnO_2 layer by simple hydrothermal-based method. To the best of our knowledge, this is the primitive example of a hybrid system where Au nanostars are coated with SnO_2 layer. Similarly, the same method was used to coat spherical and rod shaped nanoparticles with SnO_2 layer. The characterizations of Au nanoparticle-SnO_2 hybrid system were done by combination of analytical methods such as SEM-TEM analysis, EDX, XRD, UV-Vis and FTIR spectroscopy. Microscope images revealed the formation of core-shell structure of the synthesized hybrid systems. As the EDX analysis provided the primitive proof of the presence of Sn on the coating, XRD analyses more clearly revealed that the layer on Au nanoparticles is SnO_2. FTIR analysis complemented the characterization of coating on Au nanoparticles and demonstrated the existence of SnO_2 on them.

Among all studied Au nanoparticle cores, star shaped ones have been proved to have superior optical properties compared to rod and spherical shaped ones. Therefore, only Au nanostar-SnO_2 hybrid system was investigated for its potential use as SERS substrate. The results showed that Au nanostars remain their SERS activity after

SnO$_2$ coating. Even though some decrease in the enhanced Raman signal was observed after the coating, all of the vibrational modes of the probe molecule (crystalviolet) were strongly enhanced at low concentrations (e.g. 10^{-6} M) of the molecule.

The Raman enhancement factors for CV modes were estimated as 2.51x10^6 ± 0.51x10^6, 2.25x10^6 ± 0.40x10^6 for uncoated and SnO$_2$-coated nanostars, respectively. This part of the study revealed that the SnO$_2$ coated Au nanostars are very promising SERS-substrates to be used in sensing applications.

The hybrid materials synthesized in this study have potential uses not only in sensing applications but also in other applications where enhanced optical properties and stability is needed. Gold nanoparticles are very good at trapping light. On the other hand, SnO$_2$ is an attractive transparent material due to its electronic properties and has been used in many electronic applications. Therefore, all the synthesized SnO$_2$-coated Au nanoparticles in three different morphologies (sphere, rod and star) are great candidates to be used in photovoltaic devices to enhance their performances.

REFERENCES

(1)   Esenturk, E. N.; Walker, A. R. H. Surface-Enhanced Raman Scattering Spectroscopy via Gold Nanostars. *J. Raman Spectrosc.* **2009**, *40* (1), 86–91.

(2)   Kumar, P. S.; Pastoriza-santos, I.; Rodriguez-Gonzalez, Benito, F. J. G. de A.; Liz-Marzan, L. M. High-Yield Synthesis and Optical Response of Gold Nanostars. *Nanotechnology* **2008**, *19* (1), 1–6.

(3)   Kozanoglu, D.; Hazar, D.; Cirpan, A.; Nalbant, E. Power Conversion Efficiency Enhancement of Organic Solar Cells by Addition of Gold Nanostars , Nanorods , and Nanospheres. *Org. Electron.* **2013**, *14* (7), 1720–1727.

(4)   Murphy, C. J.; Sau, T. K.; Gole, A. M.; Orendorff, C. J.; Gao, J.; Gou, L.; Hunyadi, S. E.; Li, T. Anisotropic Metal Nanoparticles : Synthesis , Assembly and Optical Applications. *J. Phys. Chem. B* **2005**, *109*, 13857–13870.

(5)   Jin, Y.; Li, Q.; Li, G.; Chen, M.; Liu, J.; Zou, Y.; Jiang, K.; Fan, S. Enhanced Optical Output Power of Blue Light-Emitting Diodes with Quasi-Aligned Gold Nanoparticles. *Nanoscale Res. Lett.* **2014**, *9* (1), 7.

(6)   Huang, X.; El-Sayed, I. H.; Qian, W.; El-Sayed, M. A. Cancer Cell Imaging and Photothermal Therapy in the near-Infrared Region by Using Gold Nanorods. *J. Am. Chem. Soc.* **2006**, *128* (6), 2115–2120.

(7)   Lee, S. H.; Rusakova, I.; Ho, D. M.; Jacobson, A. J.; Lee, T. R. Monodisperse SnO_2 ‐ Coated Gold Nanoparticles Are Markedly More Stable than Analogous SiO_2 ‐ Coated Gold Nanoparticles. **2013**, 1–6.

(8)   Lee, S. H.; Hoffman, D. M.; Jacobson, A. J.; Lee, T. R. Transparent, Homogeneous Tin Oxide (SnO$_2$) Thin Films Containing SnO2 Coated Gold Nanoparticles. *Chem. Mater.* **2013**, *25* (23), 4697–4702.

(9)   Zhou, N.; Polavarapu, L.; Wang, Q.; Xu, Q.-H. Mesoporous SnO$_2$-Coated Metal Nanoparticles with Enhanced Catalytic Efficiency. *ACS Appl. Mater. Interfaces* **2015**, *7* (8), 4844–4850.

(10)   Oldfield, G.; Ung, T.; Mulvaney, P. Au@SnO$_2$ Core-Shell Nanocapacitors. *Adv. Mater.* **2010**, *12* (20), 1519–1522.

(11)   Atta, S.; Tsoulos, T. V.; Fabris, L. Shaping Gold Nanostar Electric Fields for Surface-Enhanced Raman Spectroscopy Enhancement via Silica Coating and Selective Etching. *J. Phys. Chem. C* **2016**, *120* (37), 20749–20758.

(12)   Zhan, Q.; Qian, J.; Li, X.; He, S. A Study of Mesoporous Silica-Encapsulated Gold Nanorods as Enhanced Light Scattering Probes for Cancer Cell Imaging. *Nanotechnology* **2010**, *21* (5), 55704.

(13)   Huang, C. C.; Huang, C. H.; Kuo, I. T.; Chau, L. K.; Yang, T. S. Synthesis of Silica-Coated Gold Nanorod as Raman Tags by Modulating Cetyltrimethylammonium Bromide Concentration. *Colloids Surfaces A Physicochem. Eng. Asp.* **2012**, *409* (2017), 61–68.

(14)   Walker, A. R. H.; Esenturk, E. N. Gold Nanostar @ Iron Oxide Core – Shell Nanostructures : Synthesis , Characterization , and Demonstrated Surface-Enhanced Raman Scattering Properties. *J. Nanoparticle Res.* **2013**, *19* (15), 1–10.

(15)   B, B. Introduction 1. In *Handbook of Nanotechnology*; Springer, 2010; 1–13.

(16)   Nohynek, G. J.; Lademann, J.; Ribaud, C.; Roberts, M. S. Grey Goo on the Skin? Nanotechnology, Cosmetic and Sunscreen Safety. *Crit. Rev. Toxicol.* **2007**, *37* (3), 251–277.

(17) Heiligtag, F. J.; Niederberger, M. The Fascinating World of Nanoparticle Research. *Mater. Today* **2013**, *16* (7–8), 262–271.

(18) Gole, A.; Murphy, C. J. Seed-Mediated Synthesis of Gold Nanorods: Role of the Size and Nature of the Seed. *Chem. Mater.* **2004**, *16* (19), 3633–3640.

(19) Eustis, S.; el-Sayed, M. a. Why Gold Nanoparticles Are More Precious than Pretty Gold: Noble Metal Surface Plasmon Resonance and Its Enhancement of the Radiative and Nonradiative Properties of Nanocrystals of Different Shapes. *Chem. Soc. Rev.* **2006**, *35* (3), 209–217.

(20) Murphy, C. J.; Sau, T. K.; Gole, A. M.; Orendorff, C. J.; Gao, J.; Gou, L.; Hunyadi, S. E.; Li, T. Anisotropic Metal Nanoparticles: Synthesis, Assembly, and Optical Applications. *J. Phys. Chem. B* **2005**, *109* (29), 13857–13870.

(21) Issa, B.; Obaidat, I. M.; Albiss, B. A.; Haik, Y. Magnetic Nanoparticles: Surface Effects and Properties Related to Biomedicine Applications. *Int. J. Mol. Sci.* **2013**, *14* (11), 21266–21305.

(22) Prakash, J.; Pivin, J. C.; Swart, H. C. Noble Metal Nanoparticles Embedding into Polymeric Materials: From Fundamentals to Applications. *Adv. Colloid Interface Sci.* **2015**, *226*, 187–202.

(23) Willets, K. a; Hall, W. P.; Sherry, L. J.; Zhang, X. Nanoscale Localized Surface Plasmon Resonance Biosensors. **2007**, 159-173.

(24) Burda, C.; Chen, X.; Narayanan, R.; El-sayed, M. A.; Burda, C.; Chen, X.; Narayanan, R.; El-sayed, M. A. Chemistry and Properties of Nanocrystals of Different Shapes Chemistry and Properties of Nanocrystals of Different Shapes. *Chem. Rev.* **2005**, *105* (4), 1025–1102.

(25) Wiley, B. J.; Im, S. H.; Li, Z. Y.; McLellan, J.; Siekkinen, A.; Xia, Y. Maneuvering the Surface Plasmon Resonance of Silver Nanostructures through Shape-Controlled Synthesis. *J. Phys. Chem. B* **2006**, *110* (32), 15666–15675.

(26) Horikoshi, S.; Serpone, N. Introduction to Nanoparticles. In *Microwaves in Nanoparticle Synthesis: Fundamentals and Applications*; Wiley-VCH Verlag GmbH & Co. KGaA, 2013, 1–24.

(27) Burda, C.; Chen, X.; Narayanan, R.; El-Sayed, M. A. Chemistry and Properties of Nanocrystals of Different Shapes. *Chem. Rev.* **2005**, *105*(4), 1025-1102.

(28) Willets, K. a; Hall, W. P.; Sherry, L. J.; Zhang, X. Nanoscale Localized Surface Plasmon Resonance Biosensors. In *Nanobiotechnology II: More Concepts and Applications*; John Wiley and Sons, 2007; 159–173.

(29) Daniel, M. C. M.; Astruc, D. Gold Nanoparticles: Assembly, Supramolecular Chemistry, Quantum-Size Related Properties and Applications toward Biology, Catalysis and Nanotechnology,. *Chem. Rev.* **2004**, *104* (1), 293–346.

(30) Barnes, W. L.; Dereux, A.; Ebbesen, T. W. Surface Plasmon Subwavelength Optics. *Nature* **2003**, *424* (6950), 824–830.

(31) Nehl, C. L.; Liao, H.; Hafner, J. H. Optical Properties of Star-Shaped Gold Nanoparticles. *Nano Letters* **2006**, *6* (4), 683-688.

(32) Murphy C. J., Gole A. M., Hunyadi S. E., Orendorff C. J. One-Dimensional Colloidal Gold and Silver Nanostructures. *Inorg. Chem.* **2006**, *45* (19), 7544–7554.

(33) Ralph A. Sperling, Pilar Rivera Gil, Feng Zhang, M. Z. and W. J. P. Biological Applications of Gold Nanoparticles. *Chem. Soc. Rev.* **2008**, *37*(9), 1896–1908.

(34)   Murphy, C. J.; Thompson, L. B.; Chernak, D. J.; Yang, J. A.; Sivapalan, S. T.; Boulos, S. P.; Huang, J.; Alkilany, A. M.; Sisco, P. N. Current Opinion in Colloid & Interface Science Gold Nanorod Crystal Growth : From Seed-Mediated Synthesis to Nanoscale Sculpting. *Curr. Opin. Colloid Interface Sci.* **2011**, *16* (2), 128–134.

(35)   Grzelczak, M.; Perez-Juste, J.; Mulvaney, P.; Liz-Marzan, L. M. Shape Control in Gold Nanoparticle Synthesis. *Chem. Soc. Rev.* **2008**, *37*(9), 1783–1791.

(36)   Murphy, C. J.; Thompson, L. B.; Alkilany, A. M.; Sisco, P. N.; Boulos, S. P.; Sivapalan, S. T.; Yang, J. A.; Chernak, D. J.; Huang, J. The Many Faces of Gold Nanorods. *J. Phys. Chem. Lett.* **2010**, *1*(19), 2867–2875.

(37)   Orendorff, C. J.; Sau, T. K.; Murphy, C. J. Shape-Dependent Plasmon-Resonant Gold Nanoparticles. *Small* **2006**, *2* (5), 636–639.

(38)   Hao, E.; Schatz, G. C. Electromagnetic Fields around Silver Nanoparticles and Dimers. *J. Chem. Phys.* **2004**, *120* (1), 357–366.

(39)   Thomas, K. G. *Surface Plasmon Resonances in Nanostructured Materials*; **2007**, 185-218.

(40)   Katrin Kneipp, Harald Kneipp, Irving Itzkan, Ramachandra R. Dasari, M. S. F. Ultrasensitive Chemical Analysis by Raman Spectroscopy. *Chem. Rev.* **1999**, *99*(10), 2957–2975.

(41)   Moskovits, M. Surface-Enhanced Raman Spectroscopy: A Brief Retrospective. *J. Raman Spectrosc.* **2005**, *36* (6–7), 485–496.

(42)   Nikoobakht, B.; El-sayed, M. A. Surface-Enhanced Raman Scattering Studies on Aggregated Gold Nanorods. *J. Phys. Chem. A* **2003**, *107*(18), 3372–3378.

(43)   Orendorff, C. J.; Gearheart, L.; Jana, N. R.; Murphy, C. J. Aspect Ratio Dependence on Surface Enhanced Raman Scattering Using Silver and Gold Nanorod Substrates. *Phys. Chem. Chem. Phys.* **2006**, *8* (1), 165–170.

(44) Bosnick, K.; Maillard, M.; Brus, L. Single Molecule Raman Spectroscopy at the Junctions of Large Ag Nanocrystals. *J. Phys. Chem. B* **2003**, *107* (37), 9964–9972.

(45) Toderas, F.; Baia, M.; Baia, L.; Astilean, S. Controlling Gold Nanoparticle Assemblies for Efficient Surface-Enhanced Raman Scattering and Localized Surface Plasmon Resonance Sensors. *Nanotechnology* **2007**, *18* (25), 255702.

(46) Israelsen, N. D.; Hanson, C.; Vargis, E. Nanoparticle Properties and Synthesis Effects on Surface-Enhanced Raman Scattering Enhancement Factor: An Introduction. *Sci. World J.* **2015**, *2015*(2015), 1-12.

(47) Joseph, V.; Matschulat, A.; Polte, J.; Rolf, S.; Emmerling, F.; Kneipp, J. SERS Enhancement of Gold Nanospheres of Defined Size. *J. Raman Spectrosc.* **2011**, *42* (9), 1736–1742.

(48) Sun, C.; Gao, M.; Zhang, X. Surface-Enhanced Raman Scattering (SERS) Imaging-Guided Real-Time Photothermal Ablation of Target Cancer Cells Using Polydopamine-Encapsulated Gold Nanorods as Multifunctional Agents. *Anal. Bioanal. Chem.* **2017**, *409* (20), 4915–4926.

(49) Yang, N.; You, T.-T.; Liang, X.; Zhang, C.-M.; Jiang, L.; Yin, P.-G. An Ultrasensitive near-Infrared Satellite SERS Sensor: DNA Self-Assembled Gold Nanorod/nanospheres Structure. *RSC Adv.* **2017**, *7* (15), 9321–9327.

(50) Herrera, G.; Padilla, A.; Hernandez-Rivera, S. Surface Enhanced Raman Scattering (SERS) Studies of Gold and Silver Nanoparticles Prepared by Laser Ablation. *Nanomaterials* **2013**, *3* (1), 158–172.

(51) Stamplecoskie, K. G.; Scaiano, J. C.; Tiwari, V. S.; Anis, H. Optimal Size of Silver Nanoparticles for Surface-Enhanced Raman Spectroscopy. *J. Phys. Chem. C* **2011**, *115* (5), 1403–1409.

(52) Demirtas, O. Comparative Study On Surface Enhanced Raman Scattering Activity Of Various Silver Nanostructures, METU, 2017.

(53)   Huang, Z.; Meng, G.; Huang, Q.; Chen, B.; Lu, Y.; Wang, Z.; Zhu, X.; Sun, K. Surface-Enhanced Raman Scattering from Plasmonic Ag-nanocube@Au-Nanospheres Core@satellites. *J. Raman Spectrosc.* **2017**, *48* (2), 217–223.

(54)   Behari, J. Principles of Nanoscience : An Overview. *Indian J. Exp. Biol.* **2010**, *48*(10), 1008–1019.

(55)   Sajanlal, P. R.; Sreeprasad, T. S.; Samal, A. K.; Pradeep, T. Anisotropic Nanomaterials: Structure, Growth, Assembly, and Functions. *Nano Rev.* **2011**, *2* (5883), 1–62.

(56)   Reetz, M.; Helbig, W. Size-Selective Synthesis of Nanostructured Transition Metal Clusters. *J. Am. Chem. Soc.* **1994**, *116* (16), 7401–7402.

(57)   Huang, C.; Wang, Y.; Chiu, P. Electrochemical Synthesis of Gold Nanocubes. *Mater. Lett.* **2006**, *60* (15), 1896–1900.

(58)   Tian, N.; Zhou, Z.; Sun, S. Platinum Metal Catalysts of High-Index Surfaces : From Single-Crystal Planes to Electrochemically Shape-Controlled Nanoparticles. *J. Phys. Chem. C 2008,* **2008**, *112* (50), 19801–19817.

(59)   Turkevich, J.; Stevenson, P. C.; J., H. A Study of the Nucleation and Growth Process in the Synthesis of Colloidal Gold. *Discuss. Faraday Soc.* **1951**, *11*, 55–75.

(60)   Livingston, J. D., Carpay, F. M. A. Controlled Nucleation for the Regulation of the Particle Size in Monodisperse Gold Suspensions. *Nat. Phys. Sci.* **1973**, *241*(1), 20–22.

(61)   Wuithschick, M., Birnbaum, A., Witte, S., Sztucki, M., Vainio, U., Pinna,N., Rademann, K., Emmerling, F., Kraehnert, R., Polte, J. Turkevich in New Robes: Key Questions Answered for the Most Common Gold Nanoparticle Synthesis. *ACS Nano* **2015,** *9* (7), 7052-7071.

(62) Yang, T.; Jiang, J. Embedding Raman Tags between Au Nanostar@Nanoshell for Multiplex Immunosensing. *Small* **2016**, *12* (36), 4980–4985.

(63) Li, J., Wu, Q., Wu, J. Synthesis of Nanoparticles via Solvothermal and Hydrothermal Methods. In *Handbook of Nanoparticles*; 2015; pp 295–328.

(64) Hayashi, H.; Hakuta, Y. Hydrothermal Synthesis of Metal Oxide Nanoparticles in Supercritical Water. *Materials.* **2010**, *3* (7), 3794–3817.

(65) Rajamathi, M.; Seshadri, R. Oxide and Chalcogenide Nanoparticles from Hydrothermal/solvothermal Reactions. *Curr. Opin. Solid State Mater. Sci.* **2002**, *6* (4), 337–345.

(66) Dertli, E.; Coskun, S.; Esenturk, E. N. Gold Nanowires with High Aspect Ratio and Morphological Purity: Synthesis, Characterization, and Evaluation of Parameters. *J. Mater. Res.* **2013**, *28* (2), 250–260.

(67) Kwon, K.; Lee, K. Y.; Lee, Y. W.; Kim, M.; Heo, J. Controlled Synthesis of Icosahedral Gold Nanoparticles and Their Surface-Enhanced Raman Scattering Property. *J. Phys. Chem. C* **2007**, *111* (3), 1161–1165.

(68) Jana, N. R.; Gearheart, L.; Murphy, C. J. Wet Chemical Synthesis of High Aspect Ratio Cylindrical Gold Nanorods. *J. Phys. Chem. B* **2001**, *105* (19), 4065–4067.

(69) Panikkanvalappil R. Sajanlal, Theruvakkattil S. Sreeprasad, A. K. S. and T. P. Anisotropic Nanomaterials: Structure, Growth, Assembly, and Functions. *Nano Rev.* **2011**, *2*, 1–62.

(70) Tao, A. R.; Habas, S.; Yang, P. Shape Control of Colloidal Metal Nanocrystals. *Small* **2008**, *4* (3), 310–325.

(71) Li, N.; Zhao, P.; Astruc, D. Anisotropic Gold Nanoparticles: Synthesis, Properties, Applications, and Toxicity. *Angew. Chemie - Int. Ed.* **2014**, *53* (7), 1756–1789.

(72)   Mallick, K.; Wang, Z. L.; Pal, T. Seed-Mediated Successive Growth of Gold Particles Accomplished by UV Irradiation : A Photochemical Approach for Size-Controlled Synthesis. *J. Photochem. Photobiol. A Chem.* **2001**, *140* (1), 75–80.

(73)   You, H.; Yang, S.; Ding, B.; Yang, H. Synthesis of Colloidal Metal and Metal Alloy Nanoparticles for Electrochemical Energy Applications. *Chem. Soc. Rev.* **2013**, *42* (7), 2880–2904.

(74)   Orendorff, C. J.; Gearheart, L.; Jana, R.; Murphy,C. J. Aspect Ratio Dependence on Surface Enhanced Raman Scattering Using Silver and Gold Nanorod Substrates. *Phys. Chem. Chem. Phys*. **2006**, *8*(1), 165–170.

(75)   Kimling, J.; Maier, M.; Okenve, B.; Kotaidis, V.; Ballot, H.; Plech, A. Turkevich Method for Gold Nanoparticle Synthesis Revisited. *J. Phys. Chem. B* **2006**, *110* (32), 15700–15707.

(76)   Jana, N. R.; Gearheart, L.; Murphy, C. J. Wet Chemical Synthesis of High Aspect Ratio Cylindrical Gold Nanorods. *J. Phys. Chem. B* **2001**, *105* (19), 4065–4067.

(77)   Pérez-Juste, J.; Pastoriza-Santos, I.; Liz-Marzán, L. M.; Mulvaney, P. Gold Nanorods: Synthesis, Characterization and Applications. *Coord. Chem. Rev.* **2005**, *249* (17–18), 1870–1901.

(78)   Tapan K. Sau; Murphy, C. J. Seeded High Yield Synthesis of Short Au Nanorods in Aqueous Solution. *Langmuir* **2004**, *20* (15), 6414–6420.

(79)   Nikoobakht, B.; El-sayed, M. A. Preparation and Growth Mechanism of Gold Nanorods (NRs) Using Seed-Mediated Growth Method. **2003**, *15* (10), 1957–1962.

(80)   Smith, D. K.; Korgel, B. A. The Importance of the CTAB Surfactant on the Colloidal Seed-Mediated Synthesis of Gold Nanorods. *Langmuir* **2008**, *24* (3), 644–649.

(81) Nehl, C. L.; Hafner, J. H. Shape-Dependent Plasmon Resonances of Gold Nanoparticles. *J. Mater. Chem.* **2008**, *18* (21), 2415–2419.

(82) Nikoobakht, B.; Wang, Z. L. Self-Assembly of Gold Nanorods. *J. Phys. Chem. B* **2000**, *104* (36) 8635–8640.

(83) Gole, A.; Murphy, C. J. Seed-Mediated Synthesis of Gold Nanorods : Role of the Size and Nature of the Seed. *Chem. Mater.* **2009**, *16* (19), 3633–3640.

(84) Murphy, B. C. J.; Jana, N. R. Controlling the Aspect Ratio of Inorganic Nanorods and Nanowires. *Adv. Mater.* **2002**, *14* (1), 80–82.

(85) Johnson, C. J.; Dujardin, E.; Davis, S. A.; Murphy, J.; Mann, S. Growth and Form of Gold Nanorods Prepared by Seed-Mediated , Surfactant-Directed Synthesis. *J. Mater. Chem* **2002**, *12* (6), 1765–1770.

(86) Sau, T. K.; Rogach, A. L.; Döblinger, M.; Feldmann, J. One-Step High-Yield Aqueous Synthesis of Size-Tunable Multispiked Gold Nanoparticles. *Small* **2011**, *7* (15), 2188–2194.

(87) Yuan H., Khoury C. G., Hwang H., Wilson C. M., Grant G. A., V.-D. T. NIH Public Access. *Nanotechnology* **2012**, *23(7): 075*, 211–220.

(88) Song, H. M.; Wei, Q.; Ong, Q. K.; Wei, A. Plasmon-Resonant Nanoparticles and Nanostars with Magnetic Cores: Synthesis and Magnetomotive Imaging. *ACS Nano* **2010**, *4* (9), 5163–5173.

(89) Ahmed, W.; Kooij, E. S.; van Silfhout, A.; Poelsema, B. Controlling the Morphology of Multi-Branched Gold Nanoparticles. *Nanotechnology* **2010**, *21* (12), 125605.

(90) Zhou N., Ye C., Polavarapu L. Xu Q.-H. Controlled Preparation of Au / Ag / SnO2 Core- Shell Nanoparticles Using a Photochemical Method and Applications in LSPR based Sensing. *Nanoscale* **2015**, *7* (19), 9025–9032.

(91)   Hartland, G. V. Optical Studies of Dynamics in Noble Metal Nanostructures. *Chem. Rev.* **2011**, *111* (6), 3858–3887.

(92)   Novo, C.; Funston, A. M.; Gooding, A. K.; Mulvaney, P. Electrochemical Charging of Single Gold Nanorods. *J. Am. Chem. Soc.* **2009**, *131* (41), 14664–14666.

(93)   Kelly, K. L.; Coronado, E.; Zhao, L. L.; Schatz, G. C. The Optical Properties of Metal Nanoparticles: The Influence of Size, Shape, and Dielectric Environment. *J. Phys. Chem. B* **2003**, *107* (3), 668–677.

(94)   Petrov, M. I., Melehin, V. G., Lipovskii A. A.. On the Stability of Elastic Nanoparticles. *Phys. Status Solidi B* **2016**, *249* (11), 2137-2139.

(95)   Wang, Y.; Li, L.; Wang, C. Facile Approach to Synthesize Uniform Au @ Mesoporous SnO_2 Yolk – Shell Nanoparticles and Their Excellent Catalytic Activity in 4-Nitrophenol Reduction. *J. Nanopart Res* **2016**, *18:2*, 1–11.

(96)   Remes, Z.; Kromka, A.; Vanecek, M.; Babcenko, O.; Stuchlikova, H.; Cervenka, J.; Hruska, K.; Trung, T. Q. The optical absorption of metal nanoparticles deposited on ZnO films. *Phys. Status Solidi A* **2010**, *207* (7), 1722–1725.

(97)   Garai, M.; Zhang, T.; Gao, N.; Zhu, H.; Xu, Q. Single Particle Studies on Two-Photon Photoluminescence of Gold Nanorod − Nanosphere Heterodimers. *J. Phys. Chem. C* **2016**, *120* (21), 11621–11630.

(98)   Nam, J.; Won, N.; Jin, H.; Chung, H.; Kim, S. pH-Induced Aggregation of Gold Nanoparticles for Photothermal Cancer Therapy. *J. Am. Chem. Soc.* **2009**, *131* (17), 13639–13645.

(99)   Jin, Z.; Xiao, M.; Bao, Z.; Wang, P.; Wang, J. A General Approach to Mesoporous Metal Oxide Microspheres Loaded with Noble Metal Nanoparticles. *Angew. Chem. Int. Ed. 2012,* **2012**, *51*, 6406–6410.

(100) Mei, Y.; Lu, Y.; Polzer, F.; Ballauff, M.; Drechsler, M. Catalytic Activity of Palladium Nanoparticles Encapsulated in Spherical Polyelectrolyte Brushes and Core - Shell Microgels. *Chem. Mater.* **2007**, *19* (5), 1062–1069.

(101) Tripathy, S. K.; Mishra, A.; Jha, S. K.; Wahab, R.; Al-khedhairy, A. Synthesis of thermally stable monodispersed Au@SnO2 core–shell structure nanoparticles by a sonochemical technique for detection and degradation of acetaldehyde. **2013**, *5* (6), 1456–1462.

(102) Habubi, N. F.; Mishjil, K. A.; Chiad, S. S. Structural properties and refractive index dispersion of cobalt doped SnO_2 thin films. *Indian Journal of Physics* **2013**, *87* (3), 235-239.

(103) Zhao, T.; Yu, K.; Li, L.; Zhang, T.; Guan, Z.; Gao, N.; Yuan, P.; Li, S.; Yao, S. Q.; Xu, Q. Gold Nanorod Enhanced Two-Photon Excitation Fluorescence of Photosensitizers for Two-Photon Imaging and Photodynamic Therapy. *ACS Appl. Mater. Interfaces* **2014**, *6* (4), 2700–2708.

(104) Chang, Y.; Liao, P.; Sheu, H.; Tseng, Y.; Cheng, F. Near-Infrared Light-Responsive Intracellular Drug and siRNA Release Using Au Nanoensembles with Oligonucleotide-Capped Silica Shell. *Adv. Mater.* **2012**, *24* (25), 3309–3314.

(105) Liz-marza, L. M.; Giersig, M.; Mulvaney, P. Synthesis of Nanosized Gold - Silica Core - Shell Particles. *Langmuir* **1996**, *7463* (5), 4329–4335.

(106) Zhao, H.; Yang, F.; Tong, P.; Cui, Y.; Hao, Y.; Sun, Q.; Shi, F.; Zhan, Q.; Wang, H.; Furong Zhu. Efficiency Enhancement in Organic Solar Cells by Incorporating Silica-Coated Gold Nanorods at the Buffer / Active Interface. *J. Mater. Chem. C* **2015**, *3* (38), 9859-9868.

(107) Jankovic V., Yang Y. M., You J., Dou L., Liu Y., Cheung P., Chang J. P., Yang Y.. Active Layer-Incorporated , Spectrally Nanorod-Based Light Trapping for Organic Photovoltaics. *ACS Nano* **2013**, *7* (5), 3815–3822.

(108) Chen C. H. , Su W. N., Hy S., Pan C. J. , Tsai M. C., Rick J., H. B. J. Raman Scattering Surface Signal Enhancement. *IEEE Nanotehnology Magazine*. 2014, pp 29–36.

(109) Fales, A. M.; Yuan, H.; Vo-dinh, T. Silica-Coated Gold Nanostars for Combined Surface-Enhanced Raman Scattering (SERS) Detection and Singlet-Oxygen Generation : A Potential Nanoplatform for Theranostics. *Langmuir* **2011**, *27* (19), 12186–12190.

(110) Joo, S. H.; Park, J. Y.; Tsung, C.; Yamada, Y.; Yang, P.; Somorjai, G. A. Nanocatalysts for High-Temperature Reactions. *Nat. Mater.* **2008**, *8* (2), 126–131.

(111) Shen, Q.; Jiang, J.; Liu, S.; Han, L.; Fan, X.; Fan, M. Facile Synthesis of Au-SnO$_2$ Hybrid Nanospheres with Enhanced Photoelectrochemical Biosensing. *Nanoscale* **2014**, *6* (12) 6315–6321.

(112) Dadkhah, M.; Ansari, F. Thermal Treatment Synthesis of SnO 2 Nanoparticles and Investigation of Its Light Harvesting Application. *Appl. Phys. A* **2016**, *122* (7), 1–9.

(113) Yu, Y.; Dutta, P. Journal of Solid State Chemistry Synthesis of Au / SnO 2 Core – Shell Structure Nanoparticles by a Microwave-Assisted Method and Their Optical Properties. *J. Solid State Chem.* **2011**, *184* (2), 312–316.

(114) Batzill, M.; Diebold, U.; Batzill, M.; Diebold, U. The Surface and Science of Tin Oxide. *Prog. Surf. Sci.* **2005**, *79* (2-4), 47–154.

(115) Bajaj G., Soni R. K. Synthesis of Composite Gold / Tin-Oxide Nanoparticles by Nano-Soldering. *J. Nanopart Res* **2010**, *12* (7), 2597–2603.

(116) Zhang, L.; Zhao, J.; Lu, H.; Gong, L.; Li, L.; Zheng, J.; Li, H.; Zhu, Z. High Sensitive and Selective Formaldehyde Sensors Based on Nanoparticle-Assembled ZnO Micro-Octahedrons Synthesized by Homogeneous Precipitation Method. *Sens. Actuators B* **2011**, *160* (1), 364–370.

(117) Chung, F.; Wu, R.; Cheng, F. Fabrication of a Au @ SnO_2 Core–Shell Structure for Gaseous Formaldehyde Sensing at Room Temperature. *Sensors Actuators B. Chem.* **2014**, *190* (1), 1–7.

(118) Jiang, X.; Zhang, L.; Wang, T.; Wan, Q. High Surface-Enhanced Raman Scattering Activity from Au-Decorated Individual and Branched Tin Oxide Nanowires. *J. Appl. Phys.* **2009**, *106* (10), 1-5.

(119) Zhou, N.; Polavarapu, L.; Wang, Q.; Xu, Q.-H. Mesoporous SnO_2-Coated Metal Nanoparticles with Enhanced Catalytic Efficiency. *ACS Appl. Mater. Interfaces* **2015**, *7* (8), 4844–4850.

(120) Zhao, K.; Du, G.; Luo, L.; Qin, G.; Jiang, Q.; Liu, Y.; Zhao, H. Novel multi-layered SnO2 nanoarray: self-sustained hydrothermal synthesis, structure, morphology dependence and growth mechanism. *CrystEngComm* **2015**, *17* (9), 2030–2040.

(121) Rahmi, R.; Kurniawan, F. Synthesis of SnO 2 Nanoparticles by High Potential Electrolysis. *Bull. Chem. React. Eng. Catal.* **2017**, *12* (2), 281–286.

(122) Chu, X. Preparation and Gas-Sensing Properties of SnO_2 / Graphene Quantum Dots Composites via Solvothermal Method. *J. Mater. Sci.* **2017**, *52* (16), 9441–9451.

(123) Pretsch, E.; Bühlmann, P.; Affolter, C. *Structure Determination of Organic Compounds*; 2000, 245-263.

(124) Chen, H.; Kou, X.; Yang, Z.; Ni, W.; Wang, J. Shape-and Size-Dependent Refractive Index Sensitivity of Gold Nanoparticles. *Langmuir* **2008**, *24* (10), 5233–5237.

(125) Link, S.; Mohamed, M. B. Simulation of the Optical Absorption Spectra of Gold Nanorods as a Function of Their Aspect Ratio and the Effect of the Medium Dielectric Constant. **1999**, *103* (16), 3073–3077.

(126) Hou, C.; Shi, X.-M.; Zhao, C.-X.; Lang, X.-Y.; Zhao, L.-L.; Wen, Z.; Zhu, Y.-F.; Zhao, M.; Li, J.-C.; Jiang, Q. SnO $_2$ Nanoparticles Embedded in 3D Nanoporous/solid Copper Current Collectors for High-Performance Reversible Lithium Storage. *J. Mater. Chem. A* **2014**, *2* (37), 15519.

(127) Persaud, I.; Grossman, W. E. L. Surface-Enhanced Raman Scattering of Triphenylmethane Dyes on Colloidal Silver. *J. Raman Spectrosc.* **1993**, *24* (2), 107–112.

(128) Hildebrandt, P.; Stockburger, M. Surface-Enhanced Resonance Raman Spectroscopy of Rhodamine 6G Adsorbed on. *J. Phys. Chem.* **1984**, *88* (24), 5935–5944.

(129) A. Li, Z. Baird, S. Bag, D. Sarkar, A. Prabhath, T. Pradeep, R. G. C. Using Ambient Ion Beams to Write Nanostructured Patterns for Surface Enhanced Raman Spectroscopy Using Ambient Ion Beams to Write Nanostructured Patterns for Surface Enhanced Raman Spectroscopy. *Angew. Chem. Int. Ed.* **2014**, *126* (46), 12736–12739.

(130) Evcimen, N. I.; Coskun, S.; Kozanoglu, D.; Ertas, G.; Unalan, H. E.; Esenturk, E. N. Growth of Branched Gold Nanoparticles on Solid Surfaces and Their Use as Surface-Enhanced Raman Scattering Substrates. *RSC Adv.* **2015**, *5* (123), 101656–101663.

APPENDIX A

FIGURES RELATED TO CHAPTER 3
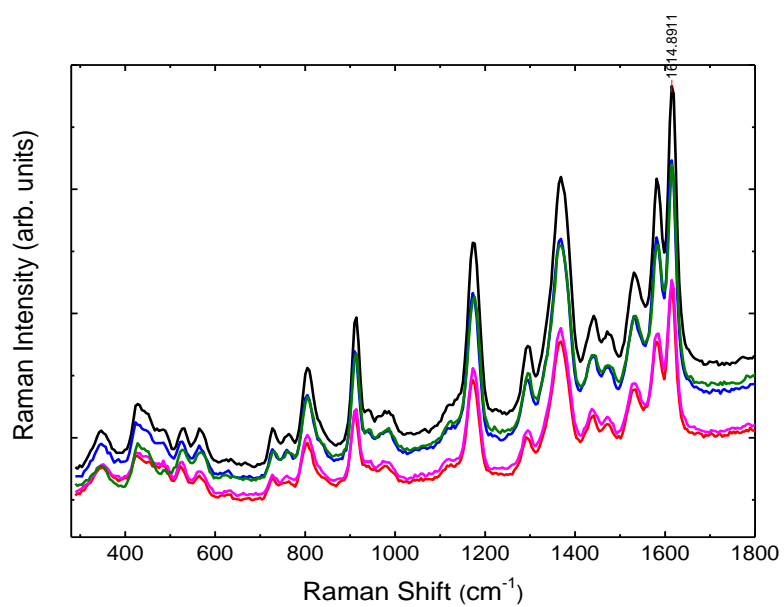
Figure A.1. SER spectra of 10^{-4} M CV on non-coated Au nanostars.
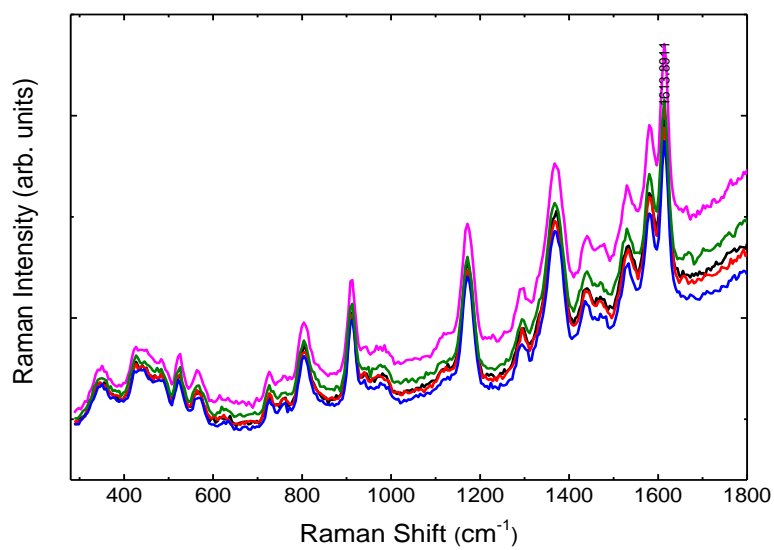
Figure A.2. SER spectra of 10^{-4} M CV on SnO_2-coated Au nanostars.
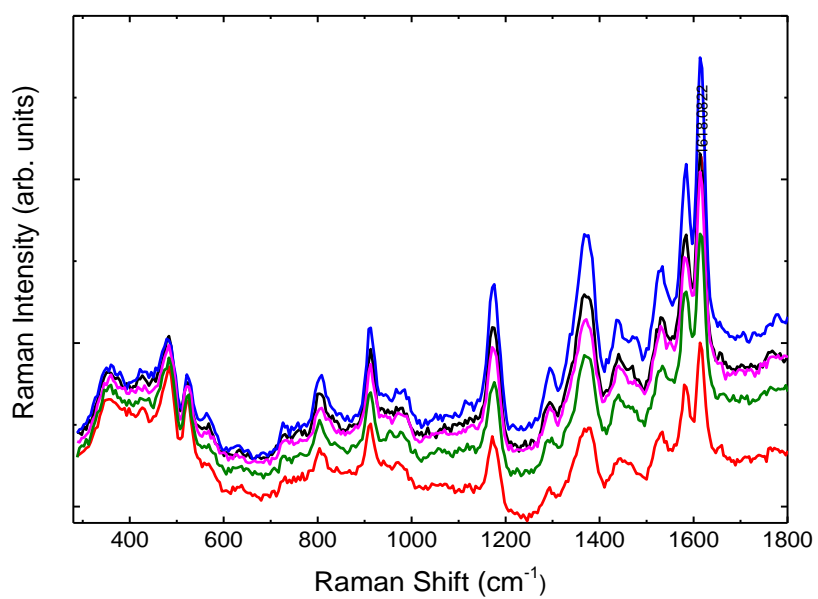
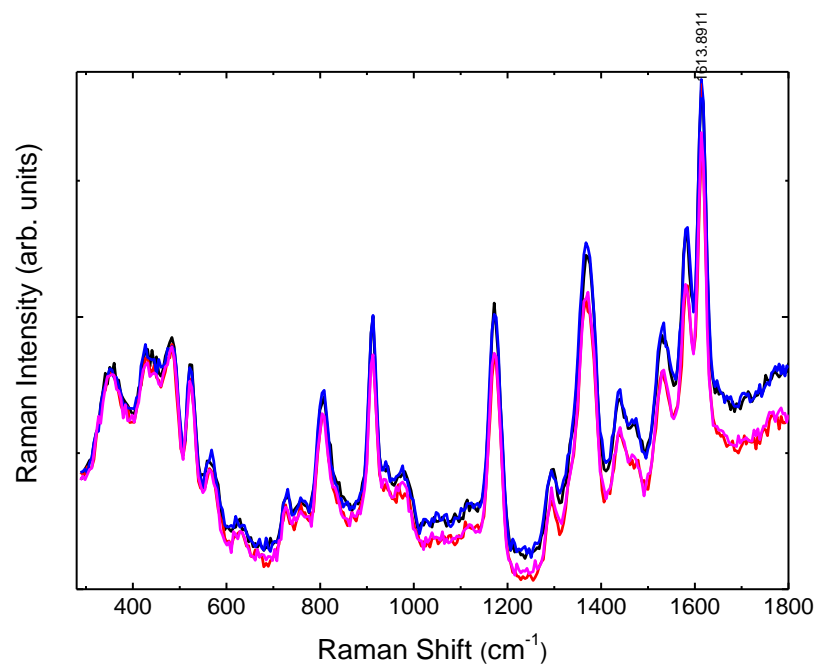**Figure A.3.** SER spectra of 10^{-5} M CV on non-coated Au nanostars.

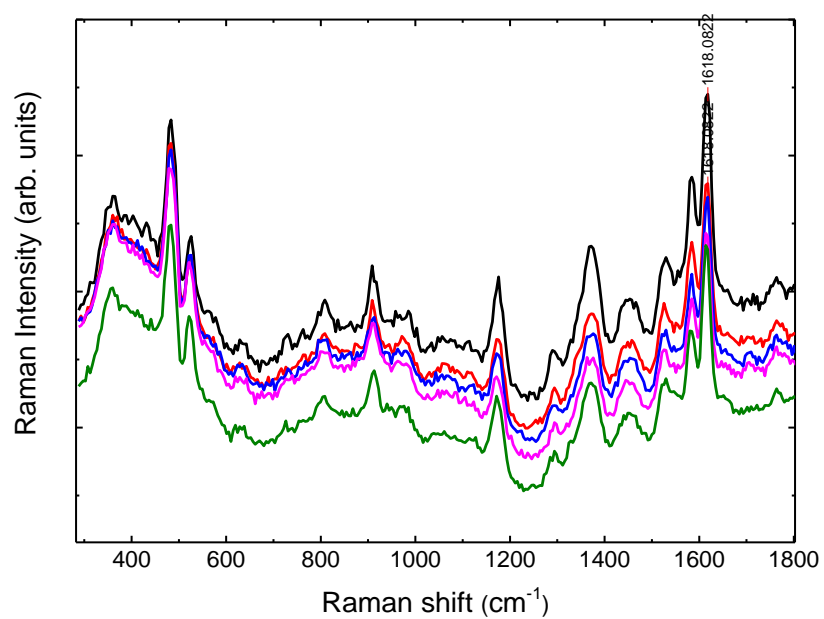**Figure A.4.** SER spectra of 10^{-5} M CV on SnO_2-coated Au nanostars.

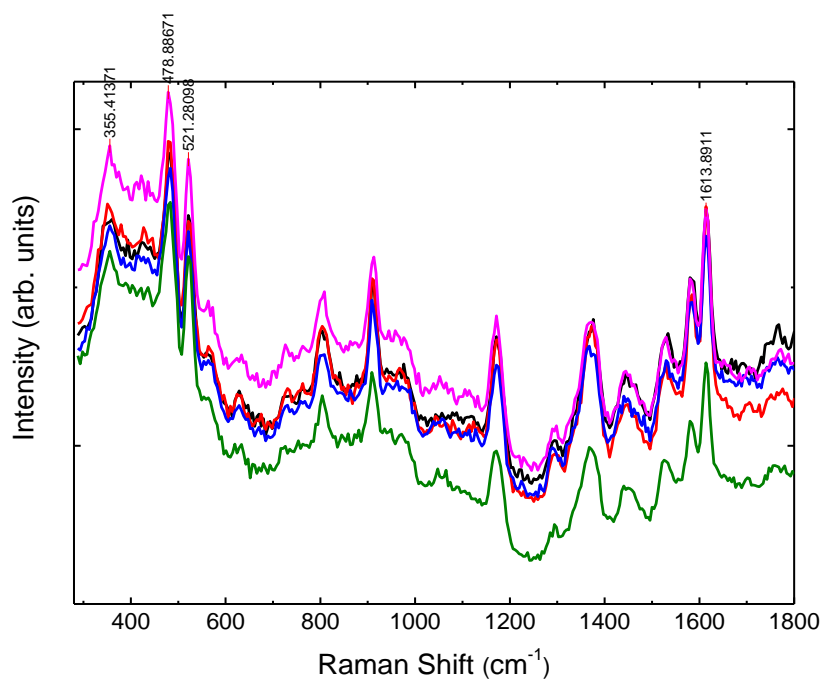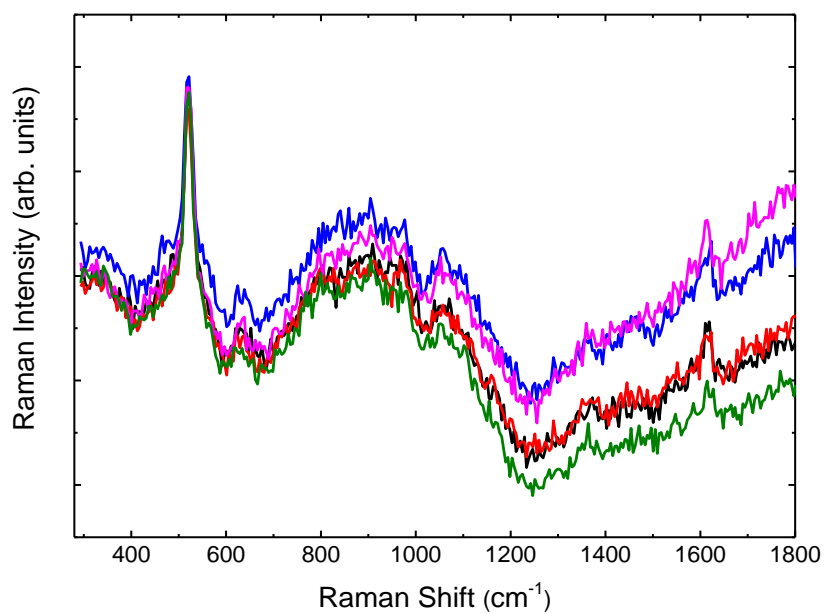**Figure A.5.** SER spectra of 10^{-6} M CV on non-coated Au nanostars

Figure A.6. SER spectra of 10^{-6} M CV on SnO_2-coated Au nanostars.

Figure A.7. SER spectra of 10^{-7} M CV on non-coated Au nanostars.
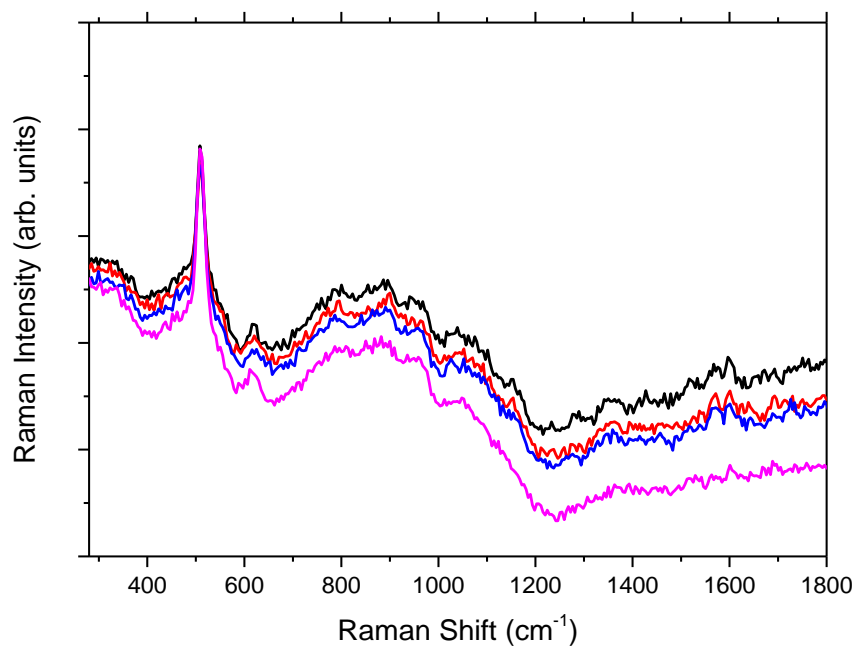
Figure A.8. SER spectra of 10^{-7} M CV on SnO_2-coated Au nanostars.
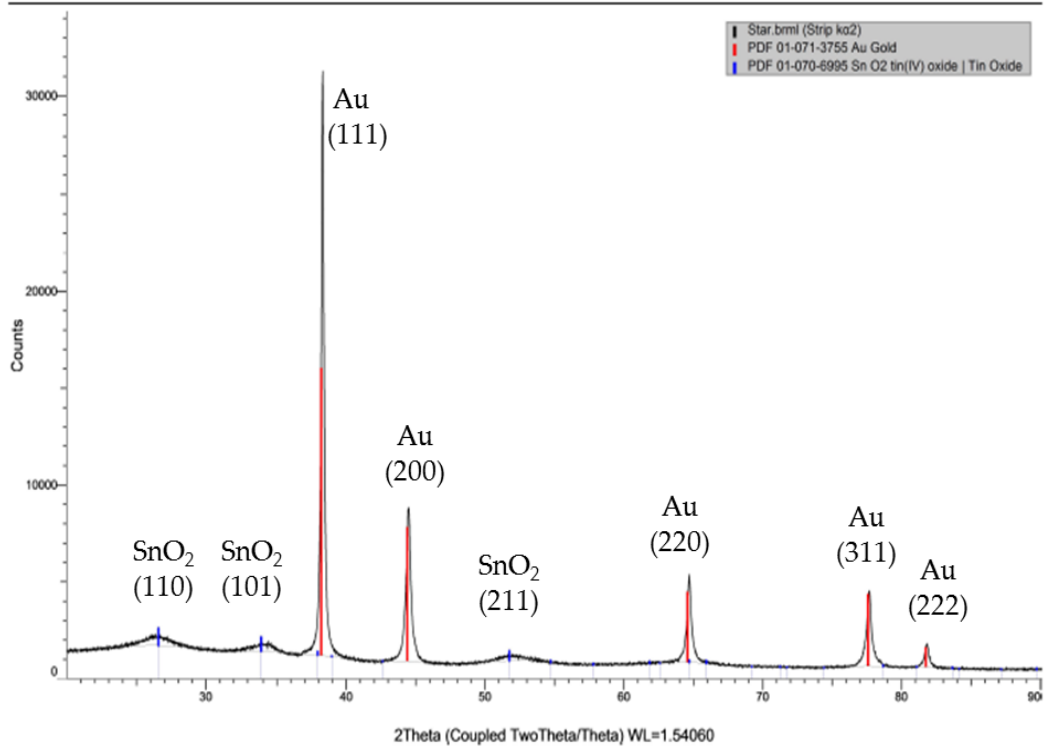
Figure A.9. XRD pattern of SnO$_2$-coated Au nanostars
(JCPDS Card No. 01-089-4898).
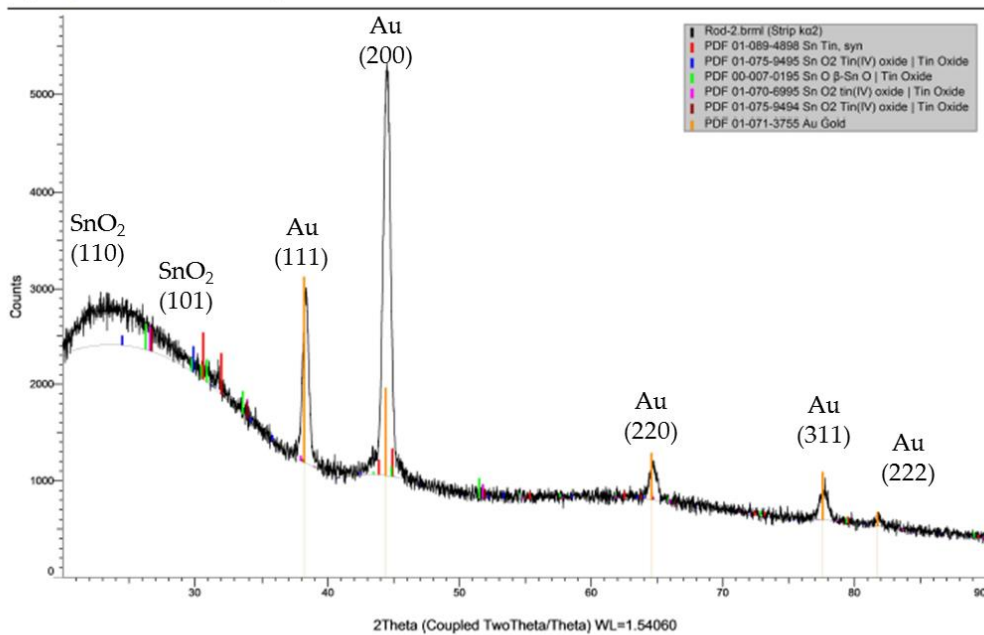
Figure A.10. XRD pattern of as-prepared SnO_2-coated Au nanorods (JCPDS Card No. 01-089-4898).

CALCULATIONS

$EF = (I_{SERS}/I_{Raman}) \times (N_{Raman}/N_{SERS})$

Raman intensity (I_{SERS}) was calculated by using the area under the peak width between 1600 and 1614 cm^{-1} for CV with 10^{-4} M concentration which was found and normalized for laser power;

I_{Raman} for 10^{-4} M CV = 15.15 cts/s

$I_{Raman} = \dfrac{15.15 \; cts/s}{160 \; mW}$

The laser spot size is 70 μm (r_z).

$A_{spot\,size} = \prod r^2 = (3,14) \times (35 \; \mu m)^2 = 3846.5 \; \mu m^2$

$A_{Au@SnO2} = \prod r^2 = (3,14) \times (225 \; nm)^2 = 158962.5 \; nm^2 = 0.16 \; \mu m^2$

$\dfrac{A_{spot\,size}}{A_{Au@SnO2}} = 24041$ molecules (number of particles on the spot size)

$N_{Raman} = C_{Raman} \times V_{probe}$

$V_{probe\,(CV)} = 4/3 \times \prod \times (35 \; \mu m) \times (35 \; \mu m) \times (70 \; \mu m) = 3.59 \times 10^{-10}$ L

$N_{Raman} = 10^{-4}$ mol/L $\times (6.02 \times 10^{23}$ molecules/mol$) \times (3.59 \times 10^{-10}$ L$)$

$N_{Raman} = 21.61 \times 10^9$ molecules (for 10^{-4} M CV)
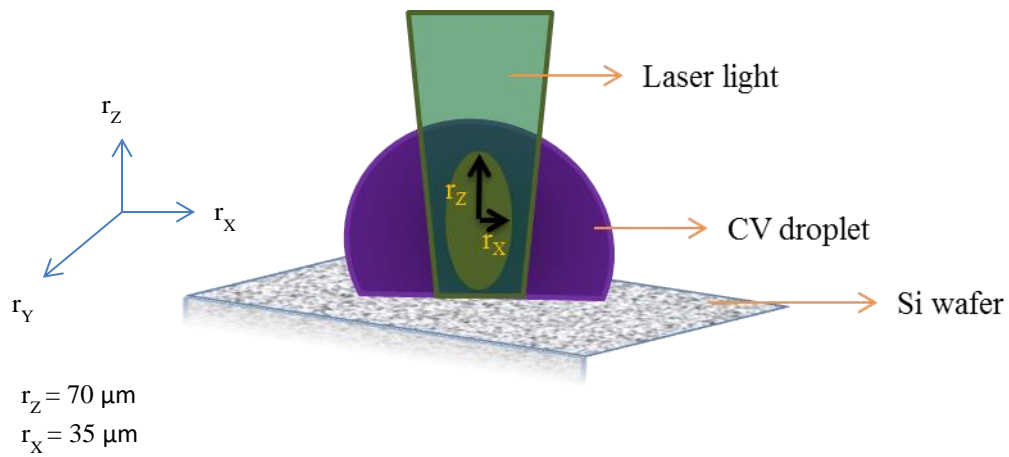
Figure B.1. Schema of CV droplet on the Si wafer.

$r_Z = 70 \ \mu m$
$r_X = 35 \ \mu m$

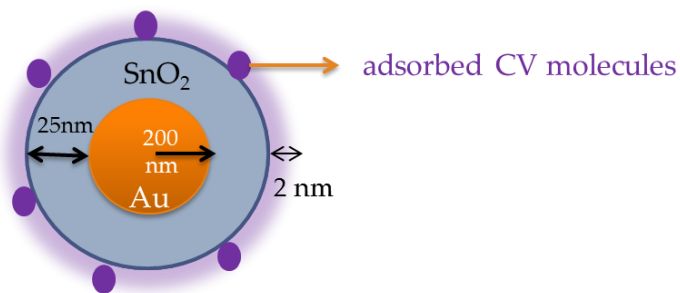**Figure B.2.** Schema of SnO$_2$-coated Au nanostar and CV molecules adsorbed on the star in max. 2 nm of distance.

$$V_{probe} = 4/3 \times \prod \times [\ (227 \ nm)^3 - (225 \ nm)^3 \ ] = 1.28 \times 10^{-18} \ L \qquad (\text{for 1 Au@SnO}_2 \text{ NS})$$

$$V_{probe} = 24041 \times 1.28 \times 10^{-18} \ L = 3.08 \times 10^{-14} \ L$$

$$N_{SERS} = C_{SERS} \times V_{probe}$$

For 10^{-4} M CV solution;

$$N_{SERS} = 10^{-4} \text{ M} \times (6.02 \times 10^{23} \text{ molecules/mol}) \times (3.08 \times 10^{-10} \text{ L})$$

$$N_{SERS} = 1854160 \text{ molecules}$$

* The same calculations were done for the other CV solutions with lower concentrations (10^{-5} M and 10^{-6} M)

$$EF = (I_{SERS}/I_{Raman}) \times (N_{Raman}/N_{SERS}) \qquad I_{SERS} = \frac{I(SERS)}{200 \; mW}$$

EF = 2.25 x 10^6 ± 0.40 x 10^6   (for SnO$_2$- coated Au nanostars)

* The similar calculation was done for non-coated Au nanostars. The radius of 1 Au nanostar is 200 nm. N_{SERS} was calculated as 1462860.

EF = 2.51 x 10^6 ± 0.51 x10^6   (for non-coated Au nanostars)